Identification and Functional Characterization of Muscle Satellite Cells in Drosophila

Rajesh Gunage, Heinrich Reichert and K. VijayRaghavan

Abstract

Work on genetic model systems such as Drosophila and mouse has shown that the fundamental mechanisms of myogenesis are remarkably similar in vertebrates and invertebrates. Strikingly, however, satellite cells, the adult muscle stem cells that are essential for the regeneration of damaged muscles in vertebrates, have not been reported in invertebrates. In this study we show role of Muscle stem cells (Gunage et al., 2014) identified in a previous study, in muscle regeneration. We show that muscle stem cells lineal descendants are present in adult muscle as small, unfused cells located superficially and in close proximity to the mature muscle fibers. Normally quiescent cells, following muscle fiber injury become mitotically active, engage in Notch-Delta signaling-dependent proliferative activity and generate lineal descendant populations, which fuse with the injured muscle fiber. In view of their strikingly similar morphological and functional features, we consider these novel cells to be Drosophila muscle satellite cells

INTRODUCTION

A great deal of insight into the cellular and molecular mechanisms of muscle development has been obtained in two powerful genetic model systems, namely the mouse and Drosophila. Despite numerous differences in the specific ways in which muscles are formed in these two organisms, there are also remarkable similarities in the fundamental developmental processes that underlie myogenesis. (Roy and VijayRaghavan, 1999; Sink, 2006; Rai et al., 2014; Bothe et al.,2016). These similarities are most clearly evident when the mechanisms of myogenesis of the large multifibrillar indirect flight muscles of Drosophila are compared to vertebrate skeletal muscles. In both cases, muscle stem cells generated during embryogenesis give rise to a large pool of muscle precursor cells called myoblasts that subsequently differentiate and fuse to produce the multinucleated syncytial cells of the mature muscle. These mechanistic similarities of myogenesis are reflected at the molecular genetic level, in that many of the key genes involved in Drosophila muscle development have served as a basis for the identification of comparable genes in vertebrate muscle development (e.g. Srinivas et al., 2007; Schnorrer et al., 2010; Abmayr and Pavlath, 2012).

In vertebrates, mature skeletal muscle cells can manifest regenerative responses to insults due to injury or degenerative disease. These regenerative events require the action of a small population of tissue specific stem cells referred to as satellite cells (Mauro 1961; Brack and Rando, 2012; Relaix and Zammit, 2012; Bothe et al., 2016). Muscle satellite cells are located superficially in the muscle fibers and surrounded by the basal lamina of the fibers. Although normally quiescent, satellite cells respond to muscle damage by proliferating and producing

myoblasts, which differentiate and fuse with the injured muscle cells. Myoblasts generated by satellite cells are also involved in the growth of adult vertebrate muscle. Given the numerous fundamental aspects of muscle stem cell biology and myogenesis that are similar in flies and vertebrates, it is surprising that muscle satellite cells have not been reported in Drosophila. Indeed, due to the apparent absence of satellite cells in adult fly muscles, it is unclear if muscle regeneration in response to injury can take place in Drosophila.

In a previous study, we showed that a small set of embryonically generated muscle-specific stem cells known as AMPs (adult muscle progenitors) give rise post-embryonically to the numerous myoblasts which fuse to form the indirect flight muscles of adult Drosophila (Gunage et al., 2014). Here we investigate the fate of the muscle stem cell-like AMPs in the adult by clonal tracing analysis and find that lineal descendants of these muscle stem cells have all of the anatomical features of muscle satellite cells. In adult muscle they remain unfused, located in close proximity to the mature muscle fibers and are surrounded by the basal lamina of the fibers. Moreover, although normally quiescent, following muscle injury they retain the potential to become mitotically active and undergo Notch signaling-dependent proliferation to generate fusion competent lineal descendants. In view of these remarkable developmental, morphological and functional features, we consider these cells to be the Drosophila equivalent of vertebrate muscle satellite cells. Thus, in flies and vertebrates the muscle stem cell lineage that generates the adult-specific muscles during normal postembryonic development is also available for adult myogenesis in muscle tissue in response to damage.

RESULTS

Two different types of cells are present in adult flight muscle

During normal postembryonic development of the indirect flight muscles, a set of approximately 250 mitotically active adult muscle precursors (AMPs) located on the epithelial surface of the wing imaginal disc generates a large number of postmitotic myoblast progeny. These myoblasts subsequently migrate and fuse with larval templates to produce the mature dorsal longitudinal muscle (DLM) fibers of the adult (Fernandes et al 1991; Gunage et al., 2014; Dhanyasi et al., 2015). The contra-lateral set of indirect flight muscles, the dorso-ventral muscles develop by the de novo fusion of AMPs to muscle founder cells (Fernandes et al 1991; Roy and VijayRaghvan 1999)

Consistent with their developmental origin by myoblast fusion with larval muscle templates, adult DLM flight muscle fibers are large multinucleated cells. This is evident in confocal optical sections through adult flight muscle fibers labeled by TOPRO (marks all nuclei) and myosin heavy chain (MHC) immunostaining, which marks myofibers .As expected, numerous nuclei, clearly located intra-cellular between individual myofibers, are seen throughout the muscle fiber (Figure 1A-B white arrow-heads; see also Figure 1 figure supplement 1 optical sections and Video 1). Interestingly, however, these optical sections also reveal nuclei located peripherally in close proximity to the muscle fiber surface (Figure 1A-B green arrowheads).

Additional co-labeling of these adult muscle fibers with Dmef2-Gal4 driving mCD8GFP (marking muscle fiber membranes) indicates that

these peripherally located nuclei belong to cells at the muscle fiber surface, which are apparently not fused with their associated muscle fiber (Figure 1C, green arrowheads). This observation is confirmed by co-staining these adult muscle fibers for expression of either Act88F (Indirect Flight muscle specific isoform of Actin) or Tropomosyin; in both cases peripherally located and apparently unfused nuclei are seen that contrast with the fused myonuclei (see Figure 1 supplement 1). To illustrate this, a 3D reconstruction of co-labeled adult muscle fibers (Video 1, 3D movie) shows a small superficially located membrane GFP-labeled cell in proximity to MHC stained muscle fibers). Figure 1D shows one of these labeled cells at higher magnification revealing that they are relatively small (length 8.5±1.4 and diameter 3.2±0.3 μm, n=50 cells from N=12 muscle preparations) wedge-shaped cells that have a prominent nucleus and are not in a myofibre network..

Scans along the z-axis through co-labeled optical sections of muscle fibers indicate that a relatively small number of these GFP-positive cells are located closely associated with the surface muscle fibers but remain unfused. To determine the numerical relationship of peripherally located unfused cells versus fused differentiated myoblasts, all optical sections (along the z-axis) of the co-labeled adult DLM muscle fibers were scored for cells associated with the surface of the muscle fibers versus cells located within the flight muscle fibers. These experiments (n=12) indicate that DLM muscle fibers have an average of 20±4 unfused cells versus an average of 700±50 fused myoblasts. Hence the ratio of unfused cells to differentiated fused myoblasts is 1:30 implying that the population of surface-associated cells is markedly smaller than the population of fused myoblasts.

Taken together, these findings indicate that two different types of cells are present in adult muscle. The first comprises the well-characterized population of differentiated myoblasts that have fused to generate the large multinuclear muscle fibers. The second comprises a novel population of small, apparently unfused cells located at the surface of the muscle fibers. In the following we will refer to these small, unfused muscle fiber-associated cells as Drosophila satellite cells.

Ultrastructural analysis of satellite cells in adult flight muscle.

To characterize the morphological features of the close association of satellite cells with the large multinucleated muscle fibers at the ultrastructural level, an electron microscopic analysis of adult DLM fibers was carried out. In electron micrographs, the mature muscle fibers are large cells containing multiple prominent nuclei, numerous organelles, as well as extensive sets of elongated myofibrils, and are surrounded by a prominent extracellular matrix (Figure 2A). In addition to these typical multinucleated muscle cells, the ultrastructural analysis also shows satellite cells as small, wedge-shaped cells located superficially and closely apposed to the large multinucleated muscle fibers (Figure 2B). These satellite cells have compact nuclei and small cytoplasmic domains with few organelles. The intact cell membrane of the satellite cells is directly adjacent to the intact muscle cell membrane demonstrating unequivocally that they are not fused with the muscle cells. They do, however, appear to be embedded in the same contiguous extracellular matrix of their adjoining muscle fiber.

In terms of their ultrastructural morphology, the satellite cells in adult flight muscle share significant characteristics with satellite cells of

vertebrate muscle. In both cases, the cells are small, mononucleated and intercalated between the cell membrane and the extracellular matrix of mature muscle fibers.

Drosophila satellite cells are lineal descendants of adult muscle precursors.

Previous work has shown that the myoblasts which fuse to generate adult muscle derive from a small set of stem cell-like AMPs (Gunage et al., 2014). Proliferating AMPs located on the larval wing disc can be identified by clonal MARCM labeling experiments using a Dmef2-Gal4 driver (Wu et al.,2006) (Figure 3A,B and video 2,3). These MARCM experiments also make it possible to label the postmitotic lineal progeny of AMPs and show that these progeny comprise the differentiated myoblasts, which subsequently fuse with founder cells during pupal stages to produce the mature multinuclear muscle fibers (Figure 3C). Given the fact that Drosophila satellite cells, like myoblasts, are labeled by the Dmef2-Gal4 driver and considering their close ultrastructural association with muscle fibers, we wondered if these satellite cells might also be lineal descendants of AMPs (Figure 3C). To investigate this, we induced MARCM (Wu et al., 2006) clones in late larval stages and recovered labeled clones in the adult muscle. (In control experiments, MARCM clones were also triggered in pupal stages and recovered in the adult to confirm that the labeled cells were not infiltrating cells that might derive from unknown proliferating cells located external to the wing disc; see Figure 3 figure supplement 1A-C).

In a first set of MARCM labeling studies, Dmef2-Gal4 was used to drive a membrane-tethered UAS-mCD8::GFP reporter; muscle cells were co-

labeled with Phalloidin and cell nuclei were co-labeled with TOPRO. Labeled cells in the adult were visualized using confocal microscopy and analysed in serial stacks of optical sections.

These clonal labeling experiments reveal the presence of satellite cells as small GFP-labeled cells closely apposed to the surface of the adult muscle fibers. Scans of optical sections along the z-axis show that these GFP-positive cells are distributed along the entire surface of the muscle fibers and located both at the interface between different muscle fibers and at the surface of individual muscle fibers but not within the muscle fibers (Figure 3E-I and J-M) (also shown in video 4). Note that, while differentiated myoblasts are also targeted in this MARCM experiment, no GFP labeled cells are visible within the adult muscle fibers since their membrane tethered GFP becomes diffuse due to incorporation into the extensive muscle fiber membrane following cell fusion (see schematic in Figure 3D).

Comparable findings were obtained in a second set of MARCM labeling experiments, in which Dmef2-Gal4 was used to drive a nuclear nls::GFP reporter label, muscle cells were co-labeled using MHC immunostaining, and cell nuclei were co-labeled with TOPRO. Scans of optical sections along the z-axis show that GFP-positive nuclei are distributed along the surface of the muscle fibers and located both at the interface between different muscle fibers and at the surface of individual muscle fibers but not within the muscle fibers (Figure 3 supplement 1D and video 5). (While the nuclei of differentiated myoblasts are also targeted in this MARCM experiment, no clonal UAS-GFP labeling is visible due to the expression of the Gal80 repressor by the unlabeled nuclei in the multinuclear cell).

These clonal MARCM labeling experiments indicate that Drosophila satellite cells are lineal descendants of AMPs. (Using the e33c-Gal4 line that marks hemocytes to drive membrane tethered GFP, we show that hemocytes are not labeled in muscles Figure 3 supplement 1E,F. Also see Fossett et al., 2003, Matova and Anderson, 2006 for expression pattern of the e33c-Gal4 in hemocytes). In contrast to myoblasts, the other type of AMP lineal progeny in the adult, satellite cells, do not fuse with the mature muscle cells but rather persist as unfused cells in the adult albeit closely associated with the mature muscle fibers.

Muscle injury results in increased mitotic activity of satellite cells

Vertebrate satellite cells are essential for muscle regeneration and repair; muscle damage results in mitotic activity of satellite cells and the proliferative production of myoblasts that rebuild compromised muscle tissue. To investigate if muscle associated cells in Drosophila can also respond to muscle injury by increased mitotic activity, we induced physical damage in adult flight muscles mechanically and subsequently probed the damaged muscle for cells showing mitotic activity.

To induce muscle damage, localized stab injury of DLM was carried out in adult flies using a small needle; care was taken to restrict damage such that only 1 or 2 muscle fibers were affected and that fibers were not severed by the injury (Figure 4A,B). DLMs damaged in this way can regenerate and in morphological respects appear normal after approximately 3 weeks (Figure 4 figure supplement 1).

To determine if damage resulted in increased mitotic activity of satellite cells, we used the mitotic marker phosphohistone-3 (PH-3) and also assayed EdU incorporation. In undamaged control muscles, evidence for mitotic activity based on PH-3 labeling was rarely observed (Figure 4C and Figure 4 figure supplement 2). In contrast, clear evidence for mitotic activity was seen in muscles 12h after physical damage had been induced. Thus, numerous PH-3 labeled nuclei were present in the damaged muscle fiber (Figure 4D). A quantification of the number of PH-3 labeled nuclei in control versus damaged muscle fibers underscores this observation (Figure 4E). Comparable results were obtained in experiments that used EdU labeling to monitor cell cycle entry. Thus, while EdU-labeled nuclei were rarely seen in undamaged control muscle fibers, they were considerably more numerous in muscle fibers 24h after damage (Figure 4 F,G). For both PH-3 and EdU labeling, evidence for increased mitotic activity was largely restricted to the damaged muscle fibers and rarely observed in undamaged muscle fibers. In contrast, within the damaged muscle fiber, evidence for increased mitotic activity was seen in nuclei along the entire extent of the fiber length.

Taken together, these findings indicate that physical damage leads to a pronounced increase in mitotic activity in cells associated with the injured flight muscle. Importantly, since the labeled nuclei in the damaged muscle were largely located at the surface of muscle fibers they correspond to the nuclei of satellite cells.

Proliferative mitotic activity of satellite cells in response to muscle injury

To further confirm that the observed increase in muscle damage-induced mitotic activity occurs in satellite cells, we performed MARCM-based clonal labeling of AMP lineal cells by using Dmef2-Gal4 to drive a membrane-tethered UAS-mCD8::GFP reporter. Clones of AMP lineages were induced in late larval stages and recovered in the adult muscles 12h after physical damage. Co-labeling of the recovered clones with PH3 showed that approximately one half of the GFP-labeled cells in the damaged muscle fibers were also PH3-positive. These PH3-positive GFP-labeled cells were satellite cells (Figure 4H-K). They were small and wedge-shaped and closely associated with the surface of the injured muscle fiber. Importantly, given the membrane-tethered nature of the GFP label, they were clearly unfused cells. These findings indicate that the AMP lineal descendants present in mature muscle as unfused satellite cells become mitotically active following injury.

Given that satellite cells become mitotically active following injury of adult muscle fibers, might some of the daughter cells they generate in the adult correspond to myoblast-like cells that can fuse with the damaged muscle? To investigate this, we used MARCM methods to visualize the lineal progeny of the mitotically active cells in injured adult muscle. In order to label only cells that were generated by mitotic activity in the adult, clones were induced in the adult 6h prior to physical injury and

recovered 24h later. (The adult stage-specific induction of clones ensures that the labeled cell lineages were generated in the adult and not in previous postembryonic stages.)

Two types of Gal4-UAS driver-reporter configurations were used in these experiments. In the first configuration, Dmef2-Gal4 was used to drive nuclear nls::GFP and muscle cells were co-labeled using MHC immunostaining while cell nuclei were co-labeled with TOPRO. In these experiments, scans along the z-axis through all co-labeled optical sections revealed nls-GFP labeled nuclei both at the surface of the damaged muscle fiber and inside of the damaged muscle fiber (Figure 4L-R and video 6). This implies that some of the daughter cells generated by satellite cells during injury-induced proliferative activity remained at the muscle cell surface while others appear to have entered muscle fiber's interior and may have fused with the injured muscle cell.

To determine if some of the adult-specific daughter cells had indeed fused with the injured muscle, comparable MARCM experiments were carried out using a second Gal4-UAS driver/reporter configuration in which Dmef2-Gal4 was used to drive a membrane-tethered mCD8::GFP and cell nuclei were co-labeled with TOPRO. In these experiments, scans along the z-axis through all co-labeled optical sections revealed both discrete GFP labeled cells that were clearly unfused as well as the type of diffuse, cloud-like GFP labeling of the muscle fiber that results when smaller cells expressing membrane-tethered GFP become incorporated into a larger multinuclear muscle fiber through cell fusion (Figure 4S-U).

The above findings were confirmed using the Fly-FUCCI system (fluorescent ubiquitination-based cell cycle indicator) to reveal putative satellite cell lineages based on CycB-RFP and E2F1-GFP reporters used together with the Dmef2 Gal4 driver (see Zielke et al., 2014). The Fly-FUCCI system is based on CycB-RFP (S-phase marker of cell cycle) and E2F1-GFP (G1-phase marker) fusion proteins that can be targeted to specific cell types using Gal4/UAS. As can be seen in figure 4 supplement 2 C,D, injured muscle fibers (D) stained for CycB-RFP (anti-RFP), E2F1-GFP (anti-GFP) as well as TOPRO-3 (marks all the nuclei) and Phalloidin (marking muscle fibre, F-actin) show a large labeled proliferating aggregate of cells derived from the AMP lineage (indicated by a white rectangle and magnified in the inset) in comparison to uninjured control muscle fibers (C) in which such labeled lineages are absent. The presence of the CycB-RFP labeled lineage in the close proximity to the injured muscle fibers (labeled by Phalloidin) confirms that mitotic activation of satellite cells occurs in injured muscle fibers in contrast to control.

Taken together, these findings indicate that AMP lineal descendants present as satellite cells in adult muscle can proliferate following muscle injury and generate lineal progeny some of which fuse with the damaged muscle fibers.

Injury induced proliferation of Drosophila satellite cells is controlled by Notch signaling

It has previously been shown that proliferative mitotic activity of AMPs during development requires Notch signaling (Gunage et al., 2014). Might the AMP lineal descendant satellite cells in adult muscle also require Notch signaling for injury-induced mitotic activity? To investigate this, we first determined if satellite cells express Notch. For this we carried out anti-Notch immunolabeling, used the Dmef2-Gal4 driver to express a membrane-tethered UAS-mCD8::GFP reporter, and co-stained with Phalloidin to label muscle fibers. (As shown in Figure 1 D-F satellite cells are devoid of F-actin and sarcomeric proteins.) These labeling studies show that satellite cells do express Notch (Figure 5A-D).

To determine if Notch expression in these cells is required for induction of mitotic activity following muscle injury, we utilized a temperature sensitive Notch allele together with PH-3 labeling; PH-3 labeling was carried out 12h after muscle injury. A quantification of the number of PH-3 labeled cells in the injured muscle of Notch temperature sensitive allele flies at restrictive (29^0C) versus permissive (17^0C) temperature is shown in figure 5 E. While numerous satellite cells were PH-3 labeled at the permissive temperature, at the restrictive temperature only few cells were PH-3-positive, implying that functional Notch is indeed required for satellite cell proliferation. (Similar results were obtained by using the chemical inhibitor DAPT, a gamma-Secretase inhibitor, to block Notch pathway activity; data not shown).

This finding was confirmed in Dmef2-driven Notch-RNAi knockdown experiments (knockdown restricted to adult stages via Gal80-ts repressor), which resulted in a dramatic reduction of PH-3 labeled cell number in injured muscle fibers as compared to controls (Figure 5F-H and, for Notch downregulation, Figure 5 supplement 1). To further confirm this finding, we performed an nls-GFP lineage analysis similar to that shown in figure 4 L-R (detailed in figure legend). In comparison to injured control muscle fibers (Figure 5I-L and video 7) injured muscle fibers experimental where Notch was specifically downregulated in satellite cells using RNAi showed significant decrease in number of nls-GFP positive cells (Figure M-N and O). Moreover, an assay of canonical Notch signaling using an NRE-GFP line (Notch Responsive Element, a GFP fusion construct of E(spl); Saj et al., 2010) shows a marked increase in labeling of satellite cells in injured muscle compared to uninjured controls (Figure 5P-R).

Taken together these results indicate that Notch signaling is required in muscle-associated satellite cells for their proliferative mitotic activity in injured muscle. To further corroborate the role of Notch in muscle repair, a functional analysis of flight responses was performed. For this, flies were subjected to a flight cylinder assay for flight initiation response (Figure 5W). After a recovery period of 48h, injured flies showed normal flight in contrast to injured flies in which downregulation of Notch function using the Dmef2 driver and N-specific RNAi was carried out (Figure 5X and Figure 5 supplement 1). Targeted Notch downregulation led to significant perturbation in the flight initiation response, indicating the importance of satellite cell lineage proliferation and fusion to restore muscle function after injury.

Proliferative activity in response to injury requires signaling between muscle fiber associated Delta and satellite cell associated Notch

Analysis of Delta expression using a Delta-GFP MIMIC line (Nagarkar-Jaiswal et al., 2015) indicates that while the Notch ligand Delta is expressed at low levels in normal flight muscle fibers, it is markedly upregulated in injured flight muscle fibers (Figure 6 A,B and B'). This suggests that upregulated expression of the Delta ligand in muscle fibers might be involved in activating the Notch receptor in satellite cells following muscle damage. In accordance with this, in Act88F-driven (muscle-specific) Delta-RNAi knockdown experiments (limited to adult stages by Gal80-ts) a marked reduction in the number of PH-3 labeled satellite cells was observed in injured muscles as compared to controls (Figure 6C-E). Similar findings were obtained when a dominant negative form of Delta was expressed using the Act88F driver in injured muscle fibers (Figure 6E).

Neuralized is an E3-ubiquitin ligase required in the Delta-Notch signal transduction process for Delta endocytosis (Skwarek et al., 2007). Analysis of a Neuralized-LacZ reporter line indicates that the muscle fiber-specific expression of Neuralized is significantly upregulated following muscle injury (Figure 6F-H). This suggests that upregulation of Neuralized in muscle fibers might be involved in the Delta-Notch signaling that results in of satellite cell proliferation following muscle damage. (Observation confirmed with immunolabeling experiments

showing that the muscle fiber-specific expression of Neuralized is significantly upregulated following muscle injury; see Figure 6 supplement 1). In accordance with this, in Act88F-driven (muscle-specific) Neuralized-RNAi knockdown experiments (limited to adult stages by Gal80-ts), a marked reduction in the number of PH-3 labeled satellite cells was observed in injured muscles as compared to controls (Figure 6I-K).

These findings imply that signaling between muscle fiber associated Delta ligand and satellite cell associated Notch receptor is required for the proliferative mitotic activity of satellite cells in response to muscle injury. Taken together with the previously mentioned experiments, our findings are in accordance with a model in which lineal descendants of muscle stem cells are present in adult muscle as superficially located satellite cells. Although normally quiescent, following muscle fiber injury these satellite cells become mitotically active, engage in Notch-Delta signaling-dependent proliferative activity and generate lineal descendant populations, which fuse with the injured muscle fiber. A simplified summary scheme of this role of satellite cells in adult muscle fibers is shown in Figure 7.

DISCUSSION

The identification and characterization of satellite cells in Drosophila indicates that stem cell lineages act not only in the development of flight muscle as reported previously (Gunage et al., 2014), but also have a role in the mature muscle of the adult. Thus, as in vertebrates, the Drosophila satellite cells are lineal descendants of the muscle-specific stem cells generated during embryogenesis, become intimately associated with adult muscle fibers and remain quiescent under normal circumstances, but become mitotically active and generate lineal progeny some of which fuse with the injured fibers following injury. The remarkable similarities in lineage, structure and function of satellite cells in flies and vertebrates imply that the role of these adult-specific muscle stem cells is evolutionarily conserved and, hence, are likely to be manifest in other animals as well. Satellite cells have been identified in a crustacean (Parhyale hawaiensis) during limb regeneration (Konstantinides et al., 2014). It will now be interesting to determine if comparable satellite cells are also present in adult musculature of other key protostome and deuterostome invertebrate phyla such as molluscs, annelids and echinoderms.

In vertebrates, satellite cells can undergo symmetric divisions which expand the stem cell pool and asymmetric divisions in which they self-renew and also generate daughter cells that differentiate into the fusion-competent myoblasts required for muscle regeneration and repair (Abmayr and Pavlath, 2012; Brack and Rando, 2012). In Drosophila, symmetric and asymmetric division modes are seen during development in the muscle stem cell-like AMPs; Notch signaling controls the initial amplification of AMPs through symmetric divisions, the switch to asymmetric divisions is mediated by Wingless regulated Numb

expression in the AMP lineage, and in both cases the wing imaginal disc acting as a niche provides critical ligands for these signaling events (Gunage et al., 2014). It will important to determine if fly satellite cells, as lineal descendants of AMPs, manifest similar cellular and molecular features in their proliferative response to muscle injury and, thus, recapitulate myogenic developmental mechanisms in the regenerative response of adult muscle. It will also be important to investigate if the mature muscle acts as a niche in this process.

In recent years, Drosophila has proven to be a powerful genetic models system for unraveling the fundamental mechanisms of muscle development and stem cell biology, and in both respects many of the findings obtained in the fly have been important for the analysis of corresponding mechanisms in vertebrates (Roy and VijayRaghavan, 1999; Abmayr and Pavlath, 2012; Egger et al., 2008; Homem and Knoblich, 2012; Jiang and Reichert, 2013). With the identification of satellite cells in Drosophila the wealth of classical and molecular genetic tools available in this model system can now be applied to the mechanistic analysis adult-specific stem cell action in myogenic homeostasis and repair. With the current set of understanding of various fusion molecules involved in early stages of myogenesis, it will be interesting to unearth possible conservation of role of fusion molecular machinery for regeneration and repair (Haralalka and Abmayr, 2010; Dhanyasi et al., 2015). Given the evidence for age and disease-related decline in satellite cell number and function in humans (e.g. Chang and Rudnicki, 2014), this type of analysis in Drosophila may provide useful information for insight into human muscle pathology.

MATERIAL AND METHODS

Fly strains, genetics and MARCM

Fly stocks were obtained from the Bloomington Drosophila Stock Centre (Indiana, USA) and were grown on standard cornmeal medium at 25°C.

For MARCM experiments mentioned in Figure 3 A, B, E-I and Figure 4H-K, S-U flies of genotype Hsflp/Hsflp; FRT 42B, Tub Gal80 were crossed to +; FRT 42B, UAS mCD8::GFP / Cyo Act-GFP ; Dmef2-Gal4 . For experiments mentioned in Figure 5I-N, flies of genotypes Hsflp/Hsflp; FRT 42B, Tub Gal80 or Hsflp/Hsflp; FRT 42B, Tub Gal80; UAS Notch RNAi were crossed to flies of genotype +; FRT 42B, UAS nls::GFP / Cyo Act-GFP ; Dmef2-Gal4. For MARCM experiments, two heat shocks of 1h each separated by 1h were given to either late third instar larvae or young adults for clonal induction. Clones were either recovered in the late larval stage for wing disc analysis or in adult stages, which were dissected and processed for flight muscles.

In knockdown and overexpression experiments the following lines were used: +; +; Dmef2-Gal4, Gal80ts, Act 88F-Gal4, Gal80ts, UAS Notch RNAi (Bloom, 35213), UAS Neur RNAi (Bloom, 26023), UAS NICD, UAS DN Delta (Bloom, 26697), UAS Delta RNAi (VDRC, 37288 and GD3720).

Other stocks used- Dl-GFP (Bloom, 59819), w1118; P{NRE-EGFP.S}5A (Bloom, 30728), Neur-LacZ (Bloom, 12124), Bloom-55121 and 55122.

Immunohistochemistry and confocal microscopy

Flight muscles were dissected from specifically staged (1-10 day old) flies and then fixed in 4% paraformaldehyde diluted in phosphate buffered saline (PBS pH-7.5). Immunostaining was performed according to (Hunt and Demontis, 2013) with few modifications. In brief, samples were then subjected to two washes of 0.3% PTX (PBS + 0.3% Triton-X) and 0.3% PBTX (PBS + 0.3% Triton-X + 0.1 %BSA) for 6h each. Primary antibody staining was performed for overnight on a shaker and secondary antibodies were added following four washes of 0.3% PTX 2h each. Excess of unbound secondary antibodies was removed at the end of 12h by two washes of 0.3% PTX 2h each following which samples were mounted in Vectashield mounting media. For immunostaining, anti-NICD (Notch intracellular C-terminal domain) (Mouse, 1:100, DSHB), anti-GFP (Chick, 1:500, Abcam, Cambridge, UK), anti-Delta (monoclonal mouse, 1:50, Hybridoma bank C594.9B), anti-MHC (Mouse, 1:100, kind gift from Dr. Richard Kripps), TOPRO-3-Iodide (1:1000, Invitrogen), Hoechst 33342 (1:500, ThermoFisher) anti-Neuralized (1:50, Rabbit)(Lai et al., 2001), Phalloidin (Alexa-488 and rhodamine conjugate, 1:500, ThermoFisher), anti-phosphohistone-3 (Rabbit, 1:100, Millipore) antibodies were used. Secondary antibodies (1:500) from Invitrogen conjugated with Alexa fluor-488, 568 and 647 were used in immunostaining procedures.

Confocal and electron microscopy

For confocal experiments, an Olympus FV 1000 confocal point scanning microscope was used for image acquisition. Images were processed using ImageJ software (Rasband WS, ImageJ U S. National Institutes of Health, Bethesda, Maryland, USA, http://imagej.nih.gov/ij/, 1997–2012). Quantification of number of actively dividing cells in PH-3 labeling experiments was performed as described in (Gunage et al., 2014).

For electron microscopic analysis the muscles were processed according to Garcia-Murillas et al., 2006. In brief, flight muscles were dissected in ice-cold fixative (2.5% glutaraldehyde in 0.1 M PIPES buffer at pH 7.4). After 10hrs of fixation at 4°C, samples were washed with 0.1M PIPES, post-fixed in 1% OsO4 (30min), and stained in 2% uranyl acetate (1hr). Samples were dehydrated in an ethanol series (50%, 70%, 100%) and embedded in epoxy. Ultrathin sections (50 nm) were cut and viewed on a Tecnai G2 Spirit Bio-TWIN electron microscope.

Muscle injury

To induce regeneration response in the flight muscle, we developed injury assay. For this, flies aged for 1, 3, 5 and 10 days were used. Flies were CO2 anaesthetized and a single stab injury was performed manually with dissection pin or tungsten needle. Care was taken so that the tungsten needle tip did not cross the hemithorax so that the damage was restricted to a minimum. The anatomical location of the injury was as shown in figure 3A. Control flies were age matched adult flies but with no injury to muscles. After injury, a recovery period of 12 h on corn meal Drosophila food was given. The flies were then processed for immunostaining of flight muscles as mentioned in the immunohistochemistry procedure. For fusion analysis flies were processed at the end of 24h.

Edu labeling for regeneration assays

EdU (5-Ethynyl-2'-deoxyuridine) incorporation allows visualization of cells actively engaged in DNA replication as well as their progeny. After brief standardization the procedure for Edu labeling is as follows. Flies were aged for 24h after eclosion subsequently starved for 12h and then

transferred on to medium containing Edu (0.2 mM final concentration) mixed cornmeal media for 3day pulse (Daul et al., 2010). Flies were injured and after a chase of 24h were processed for Edu labeling as mentioned in Gunage et al., 2014.

Flight assay

The flight test assay was performed as mentioned in Bechstedt et al., 2010 with minor modifications. Flies aged for 1-2 days were subjected to injury. Controls were uninjured flies from the same cohort. The number of flies per trial in each vial was about 10-15 and they were dropped into 1L cylinder coated with mineral oil through funnel (Figure 5W). Flies based on the flight muscle performance after falling from funnel, initiate flight and get stuck on to walls of cylinder (Figure 5W). Once stuck in the oil, flies cannot move and position of all the flies is noted at the end of each set.

Data was plotted as box plots and an unpaired t-test was performed for significance testing. The box marks the upper and lower quartiles (25 and 75%). Whiskers indicate the 10th and 90th percentiles.

Acknowledgements

REFERENCES

Abmayr, S.M., and Pavlath, G.K. (2012). Myoblast fusion: lessons from flies and mice. Development *139*, 641–656.

Bechstedt, S., Albert, J.T., Kreil, D.P., Müller-Reichert, T., Göpfert, M.C., and Howard, J. (2010). A doublecortin containing microtubule-associated protein is implicated in mechanotransduction in Drosophila sensory cilia.

Bothe, I., and Baylies, M.K. (2016). Drosophila myogenesis. Curr. Biol. *26*, R786–R791.

Brack, A.S., and Rando, T. a (2012). Tissue-specific stem cells: lessons from the skeletal muscle satellite cell. Cell Stem Cell 10, 504–514.

Chang, N.C., and Rudnicki, M. a. (2014). Satellite Cells: The Architects of Skeletal Muscle. Curr Top Dev Biol 107, 161–181.

Dhanyasi, N., Segal, D., Shimoni, E., Shinder, V., Shilo, B.-Z., VijayRaghavan, K., and Schejter, E.D. (2015). Surface apposition and multiple cell contacts promote myoblast fusion in Drosophila flight muscles. J. Cell Biol. 211 , 191–203.

Egger, B., Chell, J.M., and Brand, A.H. (2008). Insights into neural stem cell biology from flies. Philos. Trans. R. Soc. Lond. B. Biol. Sci. 363, 39–56.

Fernandes, J., Bate, M., and Vijayraghavan, K. (1991). Development of the indirect flight muscles of Drosophila. Development *113*, 67–77.

Fossett, N., Hyman, K., Gajewski, K., Orkin, S.H., and Schulz, R.A. (2003). Combinatorial interactions of serpent, lozenge, and U-shaped

regulate crystal cell lineage commitment during Drosophila hematopoiesis. Proc. Natl. Acad. Sci. U. S. A. *100*, 11451–11456.

Garcia-Murillas, I., Pettitt, T., Macdonald, E., Okkenhaug, H., Georgiev, P., Trivedi, D., Hassan, B., Wakelam, M., and Raghu, P. (2006). lazaro encodes a lipid phosphate phosphohydrolase that regulates phosphatidylinositol turnover during Drosophila phototransduction. Neuron 49, 533–546.

Gunage, R.D., Reichert, H., and VijayRaghavan, K. (2014). Identification of a new stem cell population that generates Drosophila flight muscles. Elife 3, 1–25.

Haralalka, S., and Abmayr, S.M. (2010). Myoblast fusion in Drosophila. Exp. Cell Res. 316, 3007–3013.

Homem, C.C.F., and Knoblich, J.A. (2012). Drosophila neuroblasts: a model for stem cell biology. Development *139*, 4297–4310.

Hunt, L.C., and Demontis, F. (2013). Whole-mount immunostaining of Drosophila skeletal muscle. Nat. Protoc. 8, 2496–2501.

Jiang, Y., and Reichert, H. (2013). Analysis of neural stem cell self-renewal and differentiation by transgenic RNAi in Drosophila. Arch. Biochem. Biophys. 534, 38–43.

Konstantinides, N., and Averof, M. (2014). A Common Cellular Basis for Muscle Regeneration in Arthropods and Vertebrates. Sci. 343 , 788–791.

Lai, E.C., Deblandre, G. a., Kintner, C., and Rubin, G.M. (2001). Drosophila Neuralised Is a Ubiquitin Ligase that Promotes the Internalization and Degradation of Delta. Dev. Cell 1, 783–794.

Matova, N., and Anderson, K. V (2006). Rel/NF-κB double mutants reveal that cellular immunity is central to Drosophila host defense. Proc. Natl. Acad. Sci. U. S. A. *103*, 16424–16429.

MAURO, A. (1961). Satellite cell of skeletal muscle fibers. J. Biophys. Biochem. Cytol. 9, 493–495.

Nagarkar-Jaiswal, S., Lee, P.T., Campbell, M.E., Chen, K., Anguiano-Zarate, S., Gutierrez, M.C., Busby, T., Lin, W.W., He, Y., Schulze, K.L., et al. (2015). A library of MiMICs allows tagging of genes and reversible, spatial and temporal knockdown of proteins in Drosophila. Elife *2015*.

Rai, M., Nongthomba, U., and Grounds, M.D. (2014). Skeletal Muscle Degeneration and Regeneration in Mice and Flies.

Rajaguru Aradhya, Monika Zmojdzian, Jean Philippe Da Ponte, K.J. (2015). Muscle niche-driven Insulin-Notch-Myc cascade reactivates dormant Adult Muscle Precursors in Drosophila.

Relaix, F., and Zammit, P.S. (2012). Satellite cells are essential for skeletal muscle regeneration: the cell on the edge returns centre stage. Development *139*, 2845–2856.

Roy, S., and VijayRaghavan, K. (1999). Muscle pattern diversification in Drosophila: the story of imaginal myogenesis. Bioessays 21, 486–498.

Saj, A., Arziman, Z., Stempfle, D., van Belle, W., Sauder, U., Horn, T., Dürrenberger, M., Paro, R., Boutros, M., and Merdes, G. (2010). A combined ex vivo and in vivo RNAi screen for Notch regulators in Drosophila reveals an extensive Notch interaction network. Dev. Cell 18, 862–876.

Schnorrer, F., Schönbauer, C., Langer, C.C.H., Dietzl, G., Novatchkova, M., Schernhuber, K., Fellner, M., Azaryan, A., Radolf, M., Stark, A., et al. (2010). Systematic genetic analysis of muscle morphogenesis and function in Drosophila. Nature 464, 287–291.

Skwarek, L.C., Garroni, M.K., Commisso, C., and Boulianne, G.L. (2007). Neuralized Contains a Phosphoinositide-Binding Motif Required Downstream of Ubiquitination for Delta Endocytosis and Notch Signaling. Dev. Cell 13, 783–795.

Srinivas, B.P., Woo, J., Leong, W.Y., and Roy, S. (2007). A conserved molecular pathway mediates myoblast fusion in insects and vertebrates. Nat. Genet. *39*, 781–786.

Wu, J.S., and Luo, L. (2006). A protocol for mosaic analysis with a repressible cell marker (MARCM) in Drosophila. Nat. Protoc. *1*, 2583–2589.

Zielke, N., Korzelius, J., van Straaten, M., Bender, K., Schuhknecht, G.F.P., Dutta, D., Xiang, J., and Edgar, B. a (2014). Fly-FUCCI: A versatile tool for studying cell proliferation in complex tissues. Cell Rep. *7*, 588–598.

FIGURE LEGENDS

Figure 1

Two different types of cells are present in adult flight muscle

(A) Flight muscles stained for myosin heavy chain (MHC) (Anti-MHC, red) and TOPRO (Blue) marking all the nuclei. The white arrowheads mark nuclei encapsulated by MHC-labeled myofibers, while those marked with white circle, green arrowhead are located superficially to MHC labeled myofibers. (B) Cross section of image A showing nuclei of surrounded by MHC positive muscle fibers marked by white arrowheads and nuclei at the surface of MHC positive muscle fibers marked by green arrowhead and white circle.

(C) Thoracic muscles stained for Dmef2 Gal4> UAS mCD8::GFP marking muscle membrane (Anti-GFP, Green) co-stained with (Anti-MHC, red) and TOPRO (Blue). Unfused nuclei can be seen associated with GFP-labeled membrane (white elliptical circle and green arrowheads), this is not the case for nuclei inside the muscle fibers (white arrowhead). (D) Orthogonal section of muscles stained as in D showing unfused nuclei at the muscle fiber surface associated with GFP-labeled membrane (green arrowheads) as well as nuclei in the muscle fiber without associated GFP label (white arrowhead in E). n=15, Scale bar 10μm

Figure 2

Unfused muscle-associated cells have ultrastuctural features of satellite cells.

(A, B) Transmission electron micrographs of the adult flight muscle. Myonuclei are large round double membrane structures surrounded by double membranes; outlined with white dotted lines. In A, the cytoplasm of the muscle syncytium shows distinct sarcomeres (marked as S) and mitochondria (marked as M).

(B) Electron micrograph showing mononucleated unfused cells. The intact cell membrane (marked by a green double-headed arrow) of these

cells can be distinctly seen in close apposition to muscle membrane (marked by a long red arrow) and adjacent to the basement membrane (marked by a yellow arrow) of the muscle fiber. These unfused cells contain few cytoplasmic organelles and have a wedged shaped nucleus (marked by white dotted line). n=8, Scale bar 1μm.

Figure 3

Cells of the AMP lineage persist unfused in adult muscle.

(A, B) A third instar wing imaginal disc with a MARCM clone of AMP lineage recovered from a single 15 m heat shock at 37°C, clonal induction in late third instar (120AEL). Clone shows muscle stem cell of AMP lineage (Anti-GFP, green) and green circle marks single muscle stem cell also shown in the cross section of wing disc. Muscle stem cell shows close proximity to wing disc epithelium (E) marked by white dotted line in (B). Phalloidin (red) marks F-actin in AMP lineage and TOPRO (Blue) marks all the nuclei. n=10

(C) Schematic depicting possible differential fate of muscle stem cells as compared to postmitotic myoblasts. Myoblasts from wing imaginal disc (cells from layer 2 and 3, marked by blue boxed arrow) fuse to form multinucleated flight muscles. The fate of muscle stem cells (cells adjacent to epithelium, green and marked by boxed arrow) is unknown.

(D) Schematic depicting visualization of fused versus unfused AMP lineal descendants when labeled with membrane-tethered GFP. Fusion of cells results in dilution of label in large multicellular muscle cell membrane. Label of unfused cells remains present in intact membrane enclosing a single nucleus.

(E-F) Flight muscles labeled with membrane-tethered GFP (green, anti-GFP immunolabeling), TOPRO-3 (blue) and Phalloidin (red). Single

confocal optical section; dotted lines mark muscle fiber boundaries. GFP-labeled cells represent a MARCM clone (Dmef2 driving UAS mCD8::GFP) induced in third instar (~120 h AEL) and recovered in the adult stage. Associated with the Phalloidin labeled muscle cells are unfused muscle stem cells labeled with GFP. (G-I) Insets show enlarged views of unfused cells. n=12 . (J, K) 3-D reconstruction of MARCM labeled cells and Phalloidin labeled flight muscle from same preparation as in E, F. Confocal section stack. J is a complete 3-D volume rendering and K is an orthogonal 3-D rendering of multiple optical sections shown in E-F. Unfused cells (green, anti-GFP immunolabeling) are present throughout the length of muscle and are anatomically intercalated between muscle fibers (red, phalloidin). (L) Optical orthogonal section of the same preparation as in E, F showing MARCM labeled unfused AMP lineal descendants associated with muscle fiber surfaces. Single confocal optical section. (M) Schematic of L. Scale bars 50μm. (O, P) Schematics showing muscle stem cell (Green circle with small white circle) homing to form satellite cell (Green elliptical circle). Muscle cell depicted as a long rectangle with multiple nuclei. (P) Satellite cells in the flight muscle show distribution along the length of flight muscles (Schematic based on J, K).

Figure 4

Muscle injury results in proliferative activity of satellite cells.

(A-B) Thoracic flight muscles showing the site of an injury indicated by dotted circle (white). (A) Whole mount of flight muscles labeled by Phalloidin (green) with all nuclei are labeled by TOPRO-3 (blue). Red dotted line approximately demarcates area used for further analysis of cell counting. (B) Schematic of flight muscles in fly thorax in orthogonal

view showing direction of needle (red arrow) to incur injury. Inset shows a tungsten needle used for injury. n=10

(C-D) Immunolabeling of mitotically active cells in flight muscles labeled for PH-3 (red, anti-phopsphohistone-3 immunolabeling), Phalloidin (green) and TOPRO-3 (blue) in uninjured control muscle fibers (C) and in injured muscle fibers as well as in immediately adjacent muscle fibers (D). Multiple optical sections. A marked increase in mitotically active cells is seen in injured muscle fibers as compared to controls. Red arrows indicate some of the mitotically active cells and white arrows indicate some of the mitotically inactive unfused cells. (The muscle fibers shown in panel D were located at distance of approximately 100 micrometers from the site of injury.). Scale bar 50μm and for inset 10μm.

(E) Quantification of the number of PH-3 labeled cells in control versus injured muscle. n=20.

(F, G) Edu labeling of control versus injured flight muscles. Phalloidin labeled muscle fibers showing multiple nuclei marked using TOPRO (blue) co-labeled with Edu (red) in injured muscles (G) as compared to controls (F). Red arrows indicate some of the Edu positive nuclei and white arrows indicate some of the Edu-negative nuclei. n=15.

(H-K) Injured flight muscles showing cells of MARCM labeled AMP lineages expressing a membrane-tethered GFP label, co-immunolabeled for PH-3. (Clonal labeling was achieved by using Dmef2-Gal4 to drive a membrane-tethered UAS-mCD8::GFP reporter; clones induced in late larval stages and recovered in the adult.) The clonally derived AMP lineage cells (green, anti-GFP immunolabeling; marked by red arrows) show co-localisation with PH-3 expression (red, anti-PH-3 immunolabeling) in TOPRO-labeled background (blue). n=12, Scale bar 10μm.

(L-R) Fusion of a subset of AMP lineal cells labeled by nls-GFP (nuclear localizing GFP) with injured muscle fibers. Multiple sections shown in L; single orthogonal optical sections shown in M-Q. MARCM clonal labeling with nls-GFP (Dmef2-Gal4 driving UAS-nls-GFP) was induced in the adult prior to injury and recovered one day later. Clonal analysis shows presence of GFP labeled nuclei of AMP lineal cells in the injured muscle (red, anti-MHC immunolabeling). Green arrows indicate some of these nuclei. In Q, an unfused GFP labeled cell can also be seen indicated by white circle. (R) Simplified schematic of fused versus unfused AMP lineal cells in injured muscle.

(S-U) Multiple optical sections of muscle fibers demonstrating fusion of membrane-tethered GFP positive AMP lineal cells (anti-GFP, green) to injured muscles (White dotted line). MARCM clonal labeling with membrane-tethered GFP (Dmef2-Gal4 driving UAS-mCD8::GFP) was induced in the adult 6h prior to injury and recovered one day later. All the nuclei are marked using TOPRO (blue). Red arrowheads indicate unfused lineage of satellite cell. White dotted line delineates diffuse cloud-like GFP labeling that results when smaller cells expressing membrane-tethered GFP become incorporated into a larger multinuclear muscle fiber through cell fusion. For efficient labeling flies were kept at 29^0C for 24h after injury. n=8 Scale bar 50μm. In this and all subsequent quantification results, data is presented as mean ± standard error (Student's t test); p-values < 0.01, **; p-values < 0.001, ***.

Figure 5

Activation of satellite cell proliferation is controlled by Notch signaling.

(A–D) Notch expression in flight muscles. Optical section through muscle fiber labeled with Phalloidin (white, marks F-actin) showing satellite cells (green; mCD8::GFP immunolabeled) manifesting high

Notch expression (red, anti-Notch intracellular domain immunolabeling). In (D) additional labeling with Hoechst (blue) is shown to mark all the nuclei.) The white dotted lines indicate muscle fiber boundries as demarcated by F-actin staining and the red dotted lines delimit Notch expression. A muscle fiber myonucelus (marked by red arrow head) surrounded by Phalloidin staining is devoid of both GFP and Notch expression. n= 10, scale bar 10μm.

(E) Quantification of the number of PH-3 labeled cells in injured muscle of Notch temperature sensitive allele flies at restrictive (29^0C) versus permissive (17^0C) temperature. n=12.

(F, G) Multiple optical sections of flight muscle fibers stained for mitotically active cells with PH-3 labeling (green, anti-PH-3 immunolabeling) in a anti-MHC (red, anti-MHC) and TOPRO3 (blue) labeled background in control flies (E) versus flies in which Notch is downregulated by Dmef2-Gal4, TubGal80ts > UAS Notch RNAi (F). (In this experiment, Gal80 repression was relieved post eclosion by shifting cultures from 18°C to 29°C.)

(H) Quantification of mitotically active PH3 positive satellite cells in control versus Notch downregulated flies. n=12.

(I-O) Fusion of a subset of Satellite cell lineal descendants labeled with nls-GFP (nuclear localizing GFP) to muscle fibers in control (I-K) and Notch downregulated background (M-N). Multiple sections shown in I and M; single orthogonal optical sections shown in J-L and N. MARCM clonal labeling with nls-GFP (Dmef2-Gal4 driving UAS-nls-GFP) was induced in the adult 6h prior to injury and recovered one day later. All the nuclei are marked using TOPRO (blue) and muscles are stained for myosin heavy chain (MHC) (anti-MHC, red). Green arrowheads indicate cells from Satellite cell lineage. Numerous GFP labeled nuclei can be seen in control (I-L) versus experimental where Notch was

downregulated specifically in actively dividing satellite cell using Notch specific RNAi (M-N). In L and O, an unfused GFP labeled cell can also be seen indicated by a green arrowhead. (O) Quantification of the number of nls-GFP labeled cells in uninjured versus injured muscles. n= 7 (P-V) Optical orthogonal section of flight muscle stained for NRE-GFP (Notch responsive element promoter fusion of E(Spl) driving expression of GFP), a reporter for canonical Notch signaling. In injured muscle (S-U), activation of NRE-GFP (green, anti-GFP) can be visualized in satellite cells (marked in dotted red circles); this is not seen in uninjured controls (P-R). (V) Quantification of the number of NRE-GFP labeled cells in uninjured versus injured muscles. n=8

(W, X) Flight initiation assay to test flight function recovery. (W) Schematic showing set up for flight assay comprising a 1l graduated cylinder internally coated with mineral oil and a funnel (also see methods). The green curve marks flight of a fly with good flight initiation function and a correspondingly high score in cylinder height. The red curve shows flight of a fly with faulty flight initiation function leading to lower score on cylinder height. (X) Quantification of flight initiation function using box plots. Notch function downregulation in flies during repair significantly reduces the flight recovery. Injured flies with normal levels of Notch showed complete recovery of flight at the end of 2day in comparison to undamaged controls and 5h post injury flies. Notch function was down regulated as mentioned previously in F, G. Controls used for this experiments are Dmef2-Gal4, TubGal80ts > Canton-S or Dmef2-Gal4, TubGal80ts > UAS Notch RNAi kept at 18^0C. (N=number of trials) N=3 Scale bar 50μm.

Figure 6

Delta-Neuralized signaling upregulation during muscle damage repair is crucial for Satellite cell activation.

(A, B) Optical section of flight muscle fibers in a Delta-GFP MIMIC line co-lableled by Phalloidin (marking F-actin, blue) showing upregulation of Delta-GFP level (anti-GFP, red) upon injury (B) in comparison to uninjured controls (A). n=12. (B') Quantification of signal intensity for Delta-GFP; injured muscles show significant upregulation of Delta expression in comparison to uninjured muscle (quantification in arbitrary intensity units).

(C, D) Optical section of flight muscles stained for PH-3 (green, anti-PH3 immunolabeling) and Delta expression (red, anti-Delta immunolabeling) in a TOPRO3 (blue) background in control flies (C) versus flies in which Delta is downregulated by Act88F-Gal4, TubGal80ts > UAS Delta RNAi (D). (In this experiment, Gal80 repression was relieved post eclosion by shifting cultures from 18°C to 29°C.) Delta downregulation decreases the number of mitotically active PH-3 expressing cells, some of which are indicated by green arrowheads in comparison to control.

(E) Quantification of the number of PH-3 expressing cells in control versus Delta downregulated flies; Delta downregulation is achieved by targeted Delta-RNAi knockdown as well as by targeted dominant negative Delta (DN Delta) expression. n=9

(F, G) Flight muscles stained for Neuralized (Neur) (green, anti-LacZ immunolabeling) and co-labeled by Phalloidin (red). Multiple optical sections. In comparison to controls (F), injured muscles show elevated Neuralized-lacZ positive nuclei (G), some of which are indicated by green arrowheads in comparison to control.

(H) Quantitation of Neur expression in control versus injured muscle. For quantification, the number of lac-Z positive nuclei were counted. n= 7.
(I-K) Optical section of flight muscles stained for PH-3 (green, anti-PH3 immunolabeling) and co-labeled with Phalloidin (red) and TOPRO3 (blue) in control flies (I) versus flies in which Neuralized is downregulated by Act88F-Gal4, TubGal80ts > UAS Neur RNAi (J) or Dmef2-Gal4, TubGal80ts > UAS Neur RNAi (K). Green arrowheads mark mitotically active nuclei. n=12, Scale bar 50μm

Figure 7
Simplified summary scheme of satellite cell origin during development and function in injured adult muscle fibers. Lineal descendants of muscle stem cells present in adult muscle as superficially located satellite cells are normally quiescent, however, following muscle fiber injury these cells become mitotically active, engage in Notch-Delta signaling-dependent proliferative activity and generate lineal descendant populations, which fuse with the injured muscle fiber.

Figure 1 figure supplement 1
Unfused cells are devoid of Act88F and Tropomyosin expression
(A-D) Optical section of thoracic muscle showing unfused nuclei devoid of muscle specific Act88F (isoform Actin 88F) protein. Muscles are stained for Act88F (anti GFP, green), F-actin (Phalloidin, red) and TOPRO-3-iodide (blue, marks all nuclei). Red arrows (C, D) shows nuclei peripheral to Act88F positive muscle fibers in contrast to fused myonuclei marked by white arrows (C, D). Panel D is an optical orthogonal section of panel C. n=7
(E-I) Optical section of thoracic muscle showing unfused nuclei devoid of muscle specific sarcomere protein Tropomyosin. Muscles are stained

for Tropomyosin (anti GFP, green), F-actin (Phalloidin, red) and TOPRO-3-iodide (blue marks all nuclei). Red arrows (H, I) show nuclei peripheral to Tropomyosin positive muscle fibers in contrast to fused myonuclei marked by white arrows (H, I). Panel I is an optical orthogonal section of panel H. n=10 Scale bar 50μm

Figure 3 figure supplement 1

Lineage trace of AMP lineages from pupal stage in to adult muscles

(A-C) Flight muscles labeled with membrane-tethered GFP (anti-GFP immunolabeling, green), Phalloidin (red; dotted lines mark muscle boundaries) and TOPRO-3 (labels nuclei, blue). Multiple confocal optical sections. GFP-labeled cells represent a MARCM clone (Dmef2 driving UAS mCD8::GFP) induced in pupal stage (5-10 h after puparium formation) and recovered in the adult stage. Associated with the Phalloidin labeled muscle (Outlined by red dotted line) cells are unfused satellite cells (marked by white dotted line) labeled with GFP. n=9

(D) Flight muscle fibers labeled for nls-GFP (nuclear localizing GFP, anti-GFP immunolabeling, green), MHC (anti-myosin heavy chain, red; dotted lines mark muscle boundaries) and TOPRO-3 (labels nuclei, blue). Multiple confocal optical sections. GFP-labeled cells represent a MARCM clone (Dmef2 driving UAS nls-GFP) induced as described in figure 3. Associated with the MHC labeled muscle (outlined by red dotted line) cells are unfused satellite cells (marked by white dotted line) labeled with GFP. Optical orthogonal section distinctly shows satellite cells are devoid of sarcomeric protein MHC and that their nuclei are smaller in size compared to myonuclei (i.e. nuclei in MHC positive syncytium). n=10 Scale bar 10μm

(E,F) Optical section of thoracic muscle showing absence of hemocytes. *e33c-Gal4 driver (specific for hemocytes) used to drive* UAS

mCD8::GFP *expression*. Muscles are stained for GFP (anti-GFP, green), F-actin (Phalloidin, red) and TOPRO-3-iodide (blue, marks all nuclei). In both control and experimental (injured) no GFP labeled cells were seen. n=5.

Figure 4 figure supplement 1

(A-H) Optical sections of thoracic muscle fibre showing arrangement of sarcomeric components in injured muscles post recovery of three weeks (A-D) in comparison to control (E-H). Muscle fibers are stained for MHC (anti-MHC, red), F-actin (Phalloidin, green) and TOPRO-3- iodide (marks all the nuclei). The injured muscles show a complete anatomical recovery in terms of sarcomere component organization. Scale bar 50μm n=8

Figure 4 figure supplement 2

(A-B) Multiple optical sections of thoracic muscles showing mitotic activity in injured muscles at the end of 24h. Flies of genotype Dmef2 Gal4 > UAS mCD8::GFP were injured and muscles were processed for immunolableing by anti-MHC (red) and anti-PH3 (magenta). (A) Uninjured control muscle fibers, (B) injured muscle fibers. Injured muscles (B) show a clear upregulation of mitotic activity as assayed by anti-PH3 (magenta) in unfused satellite cell (marked by membrane coupled GFP) (anti-GFP, green). The red arrow and white circle show an example of a mitotically active unfused satellite cell in (B) in contrast to a quiescent satellite cell in age matched uninjured control in (A). Scale bar 10μm n=10.

(C-D) Fly-FUCCI (fluorescent ubiquitination-based cell cycle indicator) system showing satellite cell lineage based on CycB-RFP and E2F1-GFP using Dmef2 Gal4 driver. Multiple optical sections showing uninjured and injured flight muscle fibers stained for CycB-RFP (anti-RFP, S-phase marker of cell cycle) and E2F1-GFP (anti-GFP, G1-phase marker) as well as Hoechst (marks all the nuclei, shown in the inset), and Phalloidin (marking muscle fibre F-actin, blue). Injured muscle (D) shows a large lineage (bordered with white dotted line, marked by white rectangle and shown at higher magnification in inset) as compared to control (C). The presence of CycB-RFP positive lineage (shown in rectangle) in the close proximity injured muscle fibers (marked by Phalloidin) clearly demonstrates mitotic activation of satellite cells in contrast to control muscle fibers. The injury was performed similar to that mentioned for panel B. n=6

Figure 5 figure supplement 1

Optical section of muscles showing downregulation of Notch levels using Dmef2 driver and RNAi specific to N. Muscles are immunostained for N (anti-Notch, red) and co-labeled with Phalloidin (marks F-actin, blue). Experimental animal show significant downregulation of N levels in comparison to control (Dmef2, Gal80ts> Canton-s). Muscle sarcomere apparently showed no visible phenotypes. (Similar to figure 5 F-G, in this experiment, Gal80 repression was relieved post eclosion by shifting cultures from 18°C to 29°C.)

Figure 6 figure supplement 1

Optical section of muscles showing upregulation of Neuralized. Muscle fibres are stained for Neuralized (anti-Neur, red) and Phalloidin (marks F-actin, green). Injured muscles (A-C) show significant upregulation of

Neuralized expression in comparison to uninjured muscles (Quantification in arbitrary intensity units) (E-G and H).

Video 1. 3-D reconstruction of flight muscles. Muscle labeled with myosin heavy chain (anti-MHC, red) shows satellite cells in close apposition marked by Dmef2> mCD8 GFP (anti-GFP, green). TOPRO (blue) marks all the nuclei. The nucleus of satellite cell is distinctly labeled with membranous GFP (marked by green arrow) (related to Figure 1).

Video 2. 3-D reconstruction showing optical orthogonal section of wing imaginal disc. MARCM labeled Muscle stem cells (anti-GFP, green) (marked by green arrow) in close apposition to epithelium niche (Phalloidin, red) (related to Figure 3).

Video 3. Movie of confocal optical sections showing MARCM labeled wing imaginal disc. Numerous Muscle stem cell (anti-GFP, green) shows uniform distribution on adaxial surface of epithelial niche (prominently labeled with Phallodin, red) (related to figure 3).

Video 4. Movie of confocal optical sections of adult muscles showing MARCM labeled satellite cells (related to figure 3). Membranous GFP (anti-GFP, green) clearly demarcate the boundary of satellite cell (marked by green arrow) from muscle fibre (Phalloidin, red). Satellite cells in this reconstruction can be seen distributed randomly throughout the length of muscle fibre.

Video 5. 3-D reconstruction of multiple optical sections of uninjured muscles. Satellite cells marked by MARCM labeling using nls-GFP (nuclear localization signal-Green fluorescent protein) (marked by green arrow) and muscle labeled using myosin heavy chain (anti-MHC, blue). TOPRO marks all the nuclei (red).

Video 6. Movie showing 3-D reconstruction MARCM labeled lineage of satellite cell in injured muscles (marked by green arrow) (Related to figure 4).

Video 7. Movie showing 3-D reconstruction MARCM labeled lineage of satellite cell in injured muscles (Related to figure 5). Multiple nls-GFP labeled satellite cell lineages (marked by green arrows) can be seen fused with muscle labeled using myosin heavy chain (anti-MHC, red).

Figure 1

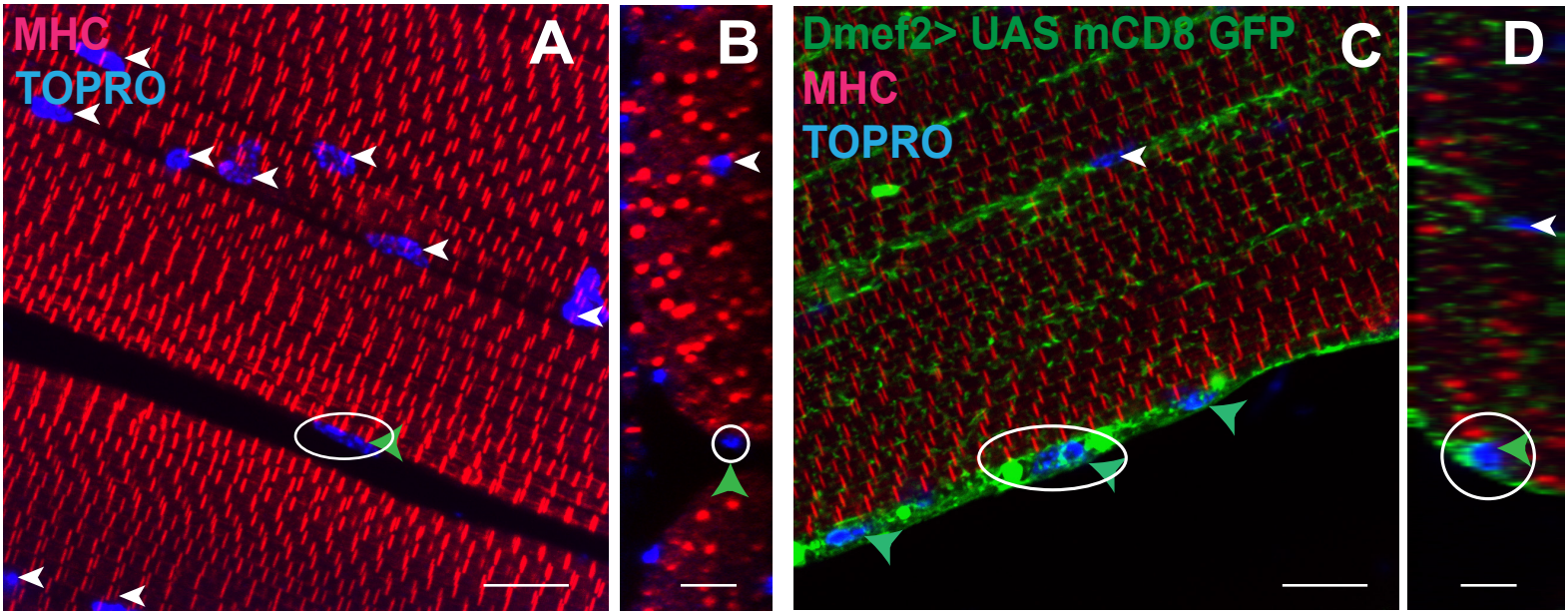

Figure 2

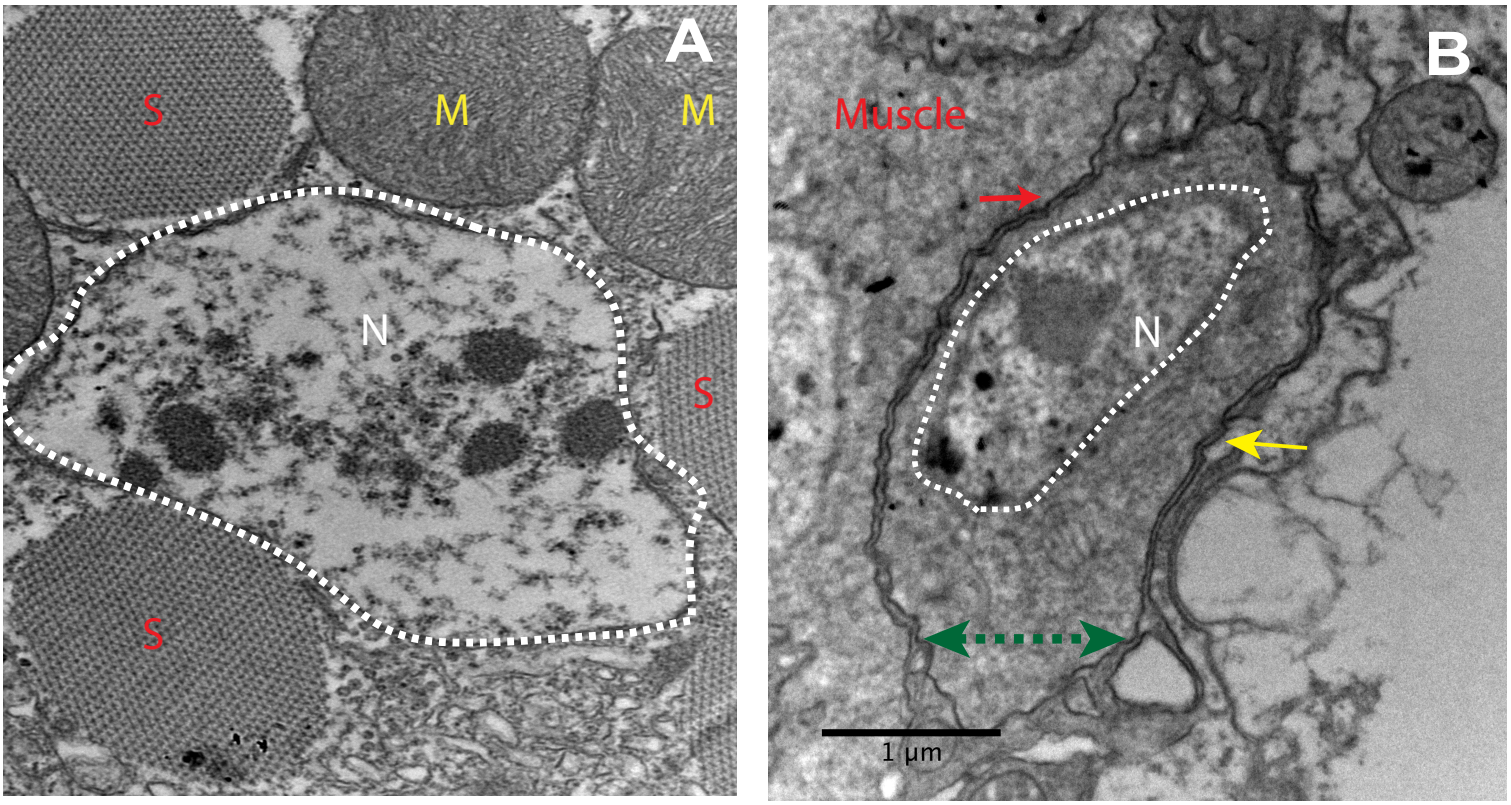

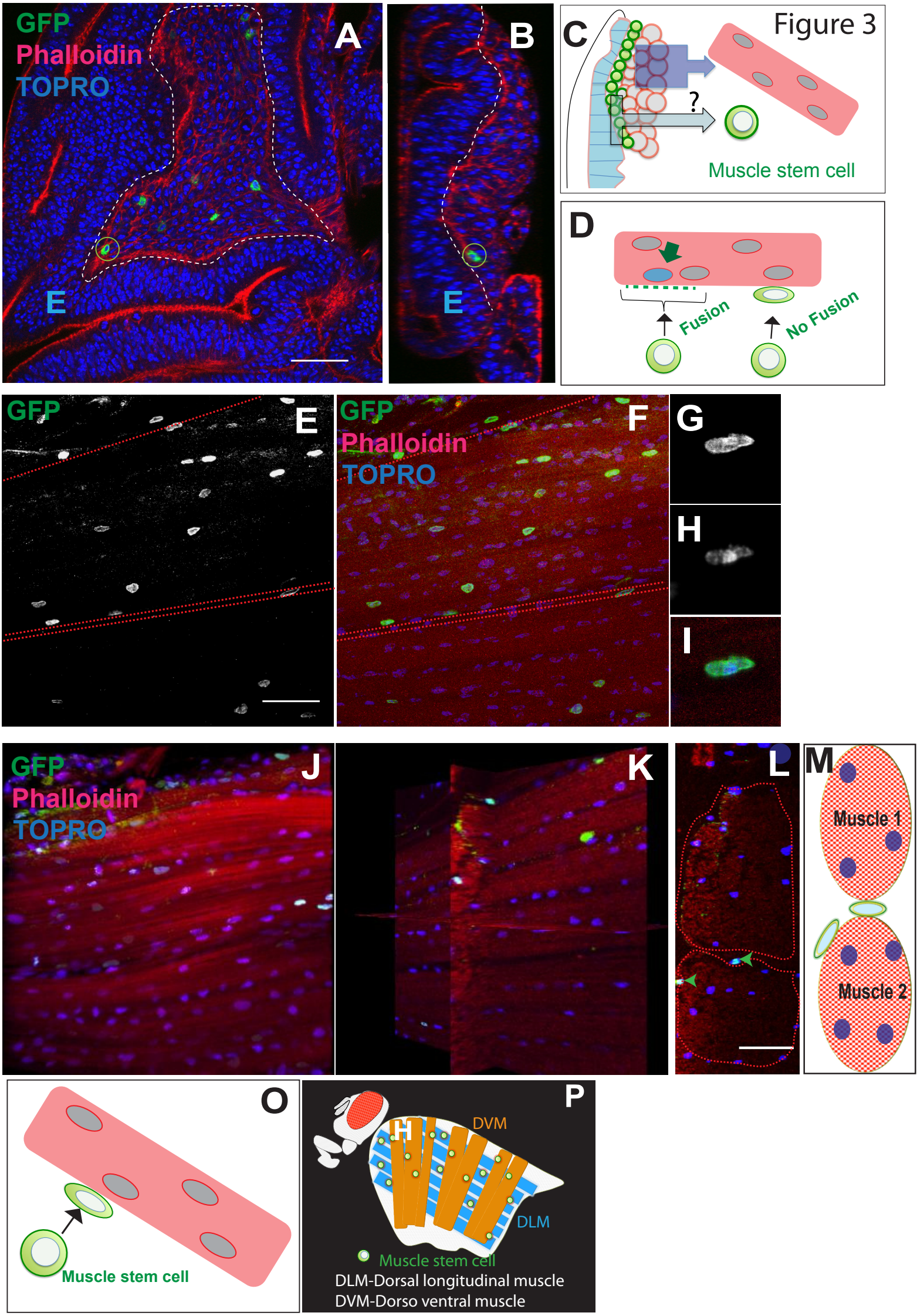
Figure 3
GFP
Phalloidin
TOPRO
A
B
C
D
E
?
Muscle stem cell
Fusion
No Fusion
F
G
H
I
J
K
L
M
Muscle 1
Muscle 2
O
P
DVM
DLM
Muscle stem cell
DLM-Dorsal longitudinal muscle
DVM-Dorso ventral muscle

Figure 4

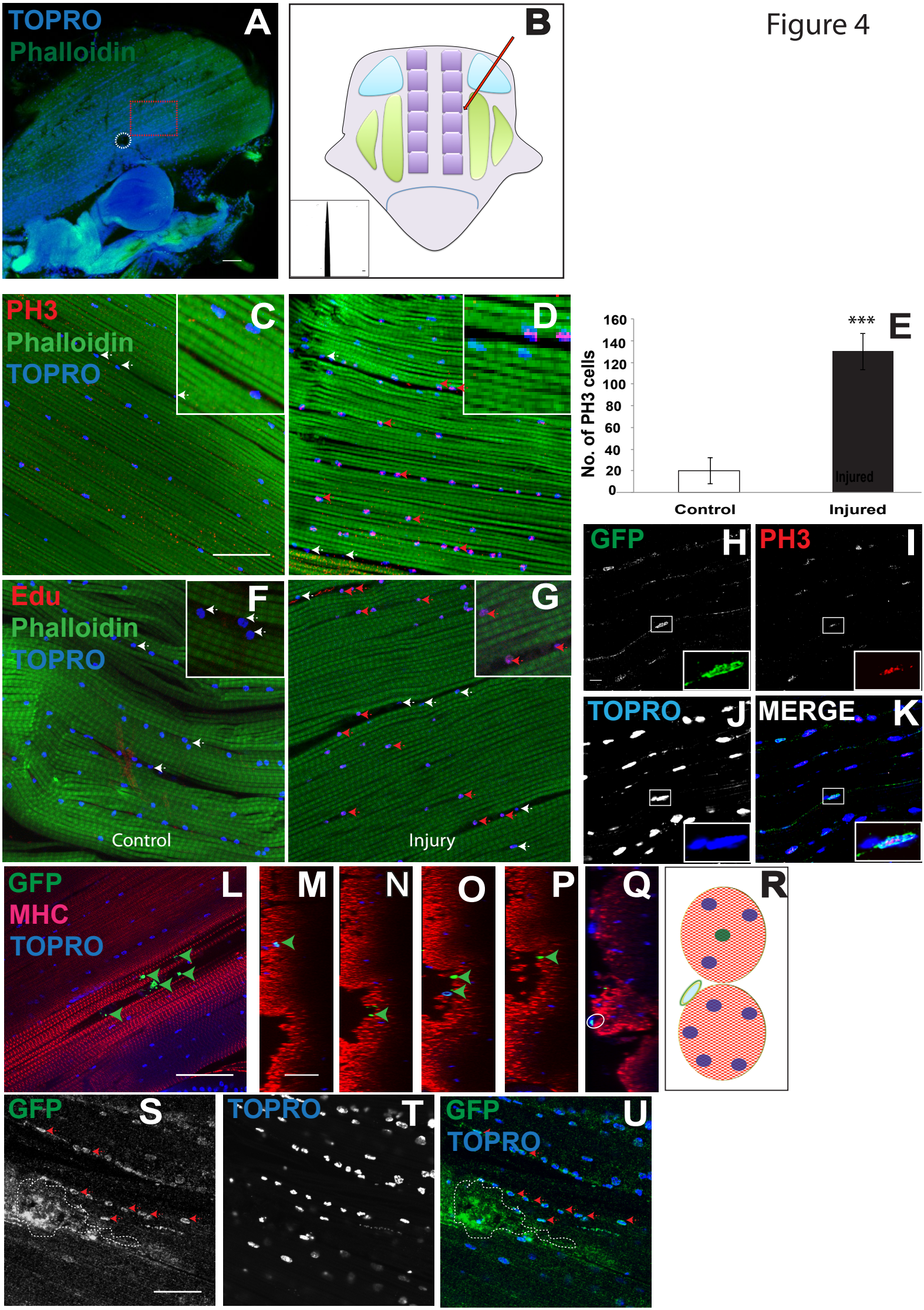
TOPRO
Phalloidin
A
B
PH3
Phalloidin
TOPRO
C
D
***
E
No. of PH3 cells
160
140
120
100
80
60
40
20
0
Control
Injured
Injured
Edu
Phalloidin
TOPRO
F
G
Control
Injury
GFP
H
PH3
I
TOPRO
J
MERGE
K
GFP
MHC
TOPRO
L
M
N
O
P
Q
R
GFP
S
TOPRO
T
GFP
TOPRO
U

Figure 5

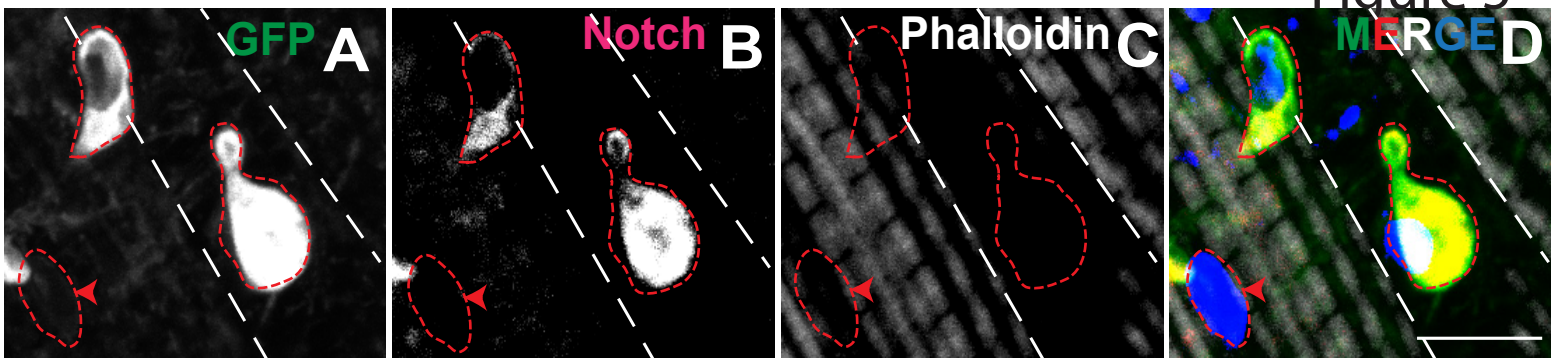
GFP
A
Notch
B
Phalloidin
C
MERGE
D

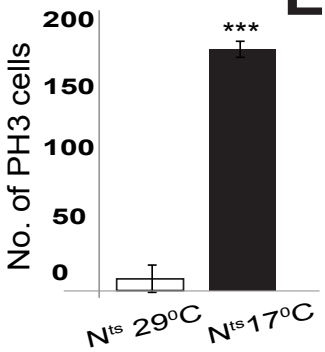
E
No. of PH3 cells
200
150
100
50
0
***
Nts 29°C
Nts17°C

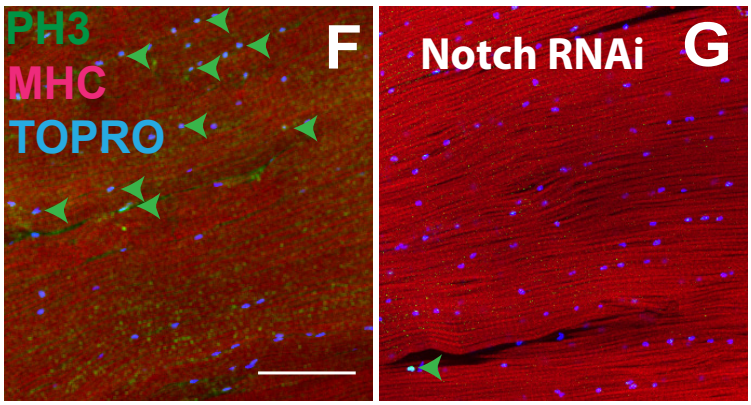
PH3
MHC
TOPRO
F
Notch RNAi
G

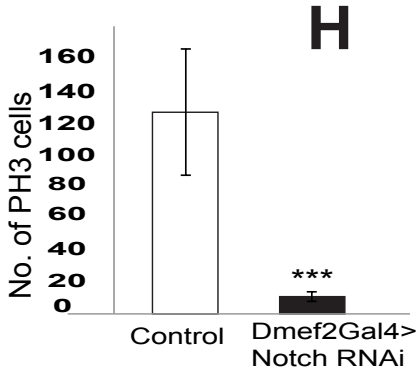
H
No. of PH3 cells
160
140
120
100
80
60
40
20
0
***
Control
Dmef2Gal4>
Notch RNAi

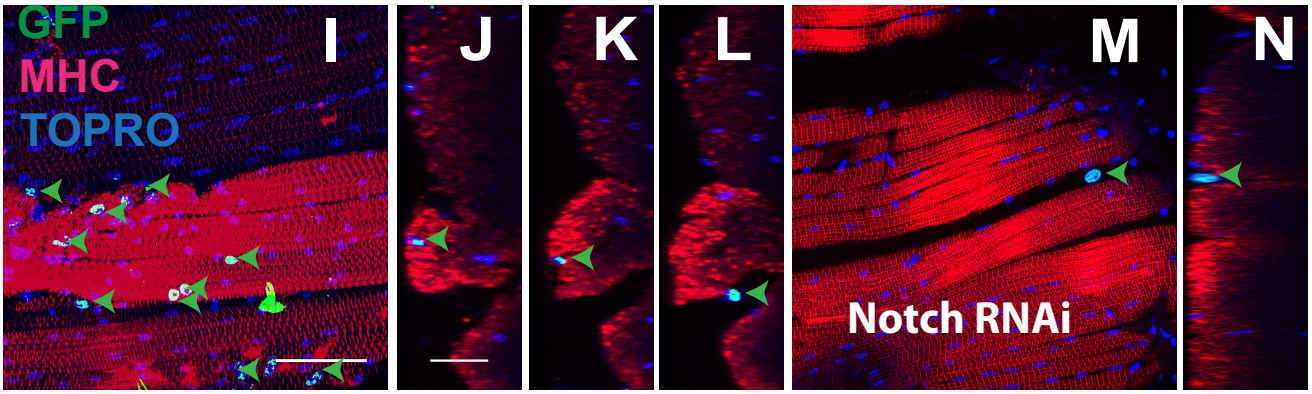
GFP
MHC
TOPRO
I
J
K
L
M
N
Notch RNAi

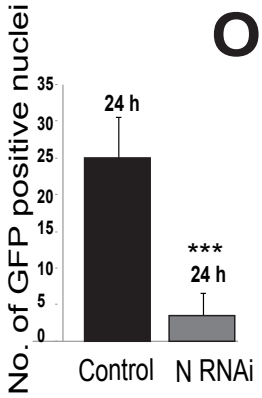
O
No. of GFP positive nuclei
35
30
25
20
15
10
5
0
24 h
***
24 h
Control
N RNAi

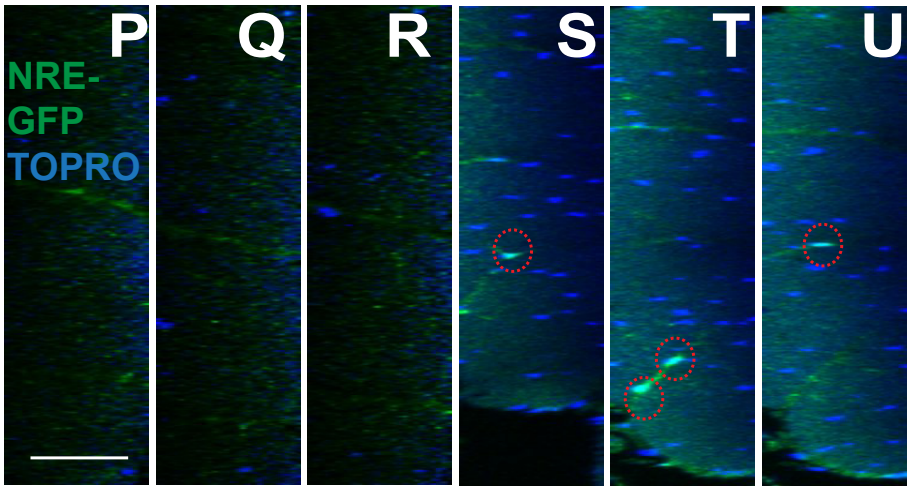
P
Q
R
S
T
U
NRE-
GFP
TOPRO

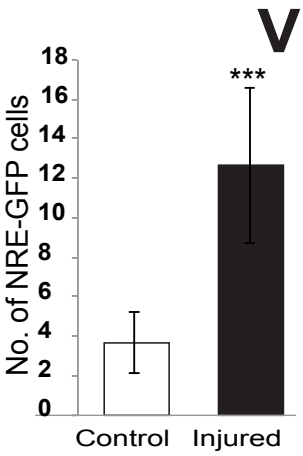
V
No. of NRE-GFP cells
18
16
14
12
10
8
6
4
2
0
***
Control
Injured

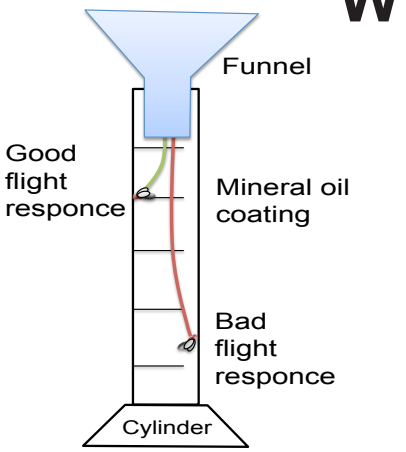
W
Funnel
Good
flight
responce
Mineral oil
coating
Bad
flight
responce
Cylinder

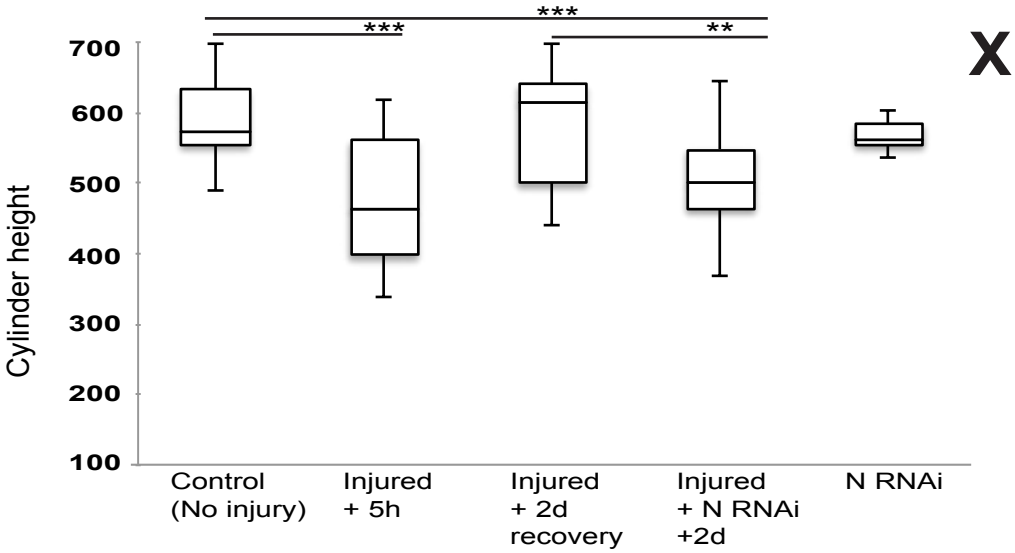
X
Cylinder height
700
600
500
400
300
200
100
***
***
**
Control
(No injury)
Injured
+ 5h
Injured
+ 2d
recovery
Injured
+ N RNAi
+2d
N RNAi

Figure 6

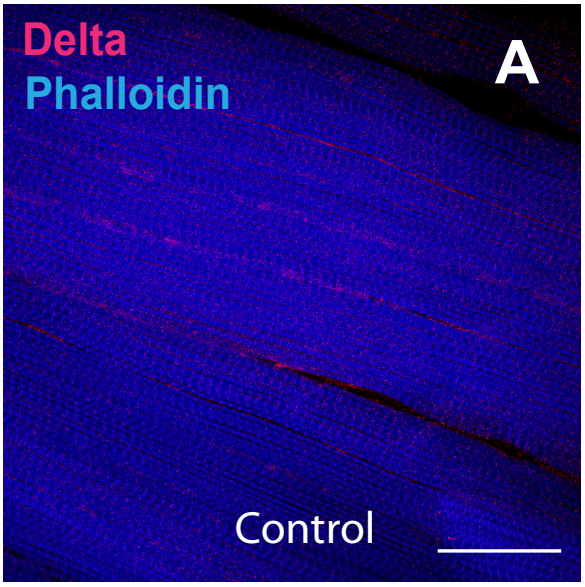
Delta
Phalloidin
A
Control

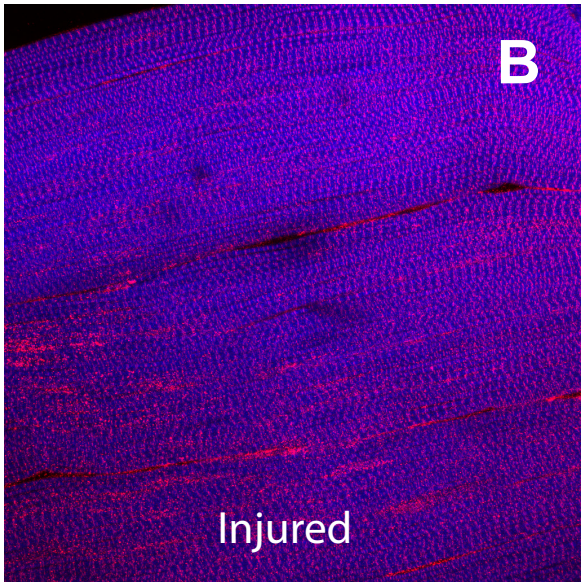
B
Injured

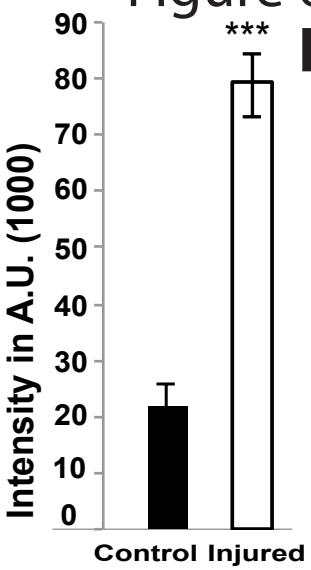
B'
Intensity in A.U. (1000)
90
80
70
60
50
40
30
20
10
0
***
Control
Injured

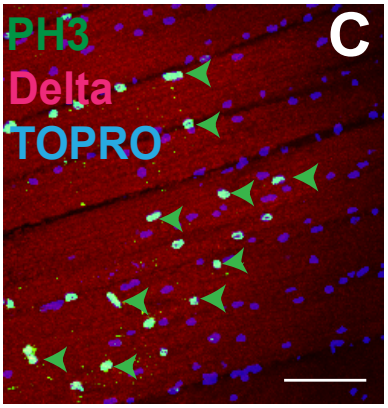
PH3
Delta
TOPRO
C

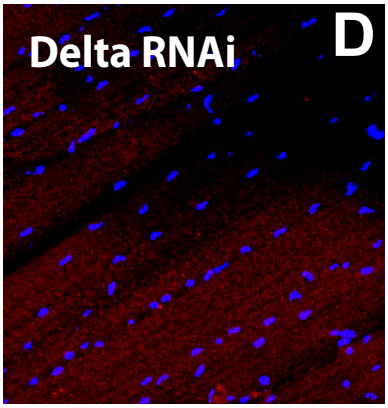
Delta RNAi
D

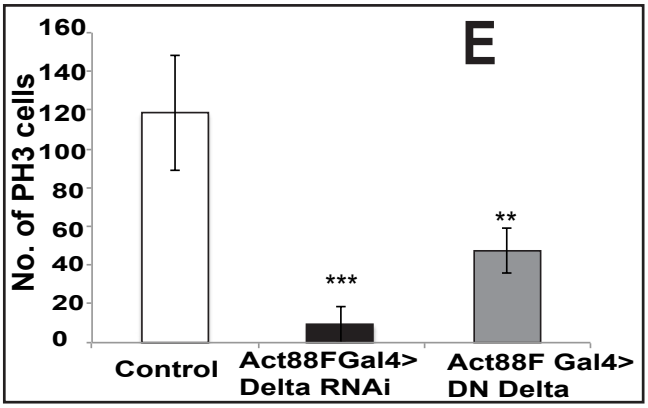
E
No. of PH3 cells
160
140
120
100
80
60
40
20
0
***
**
Control
Act88FGal4>
Delta RNAi
Act88F Gal4>
DN Delta

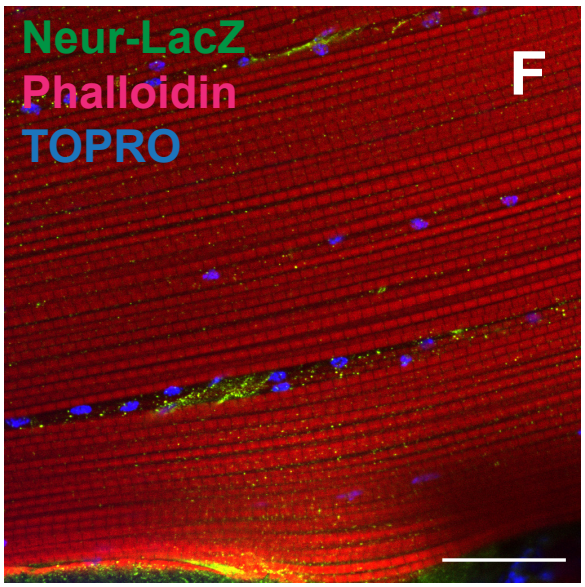
Neur-LacZ
Phalloidin
TOPRO
F

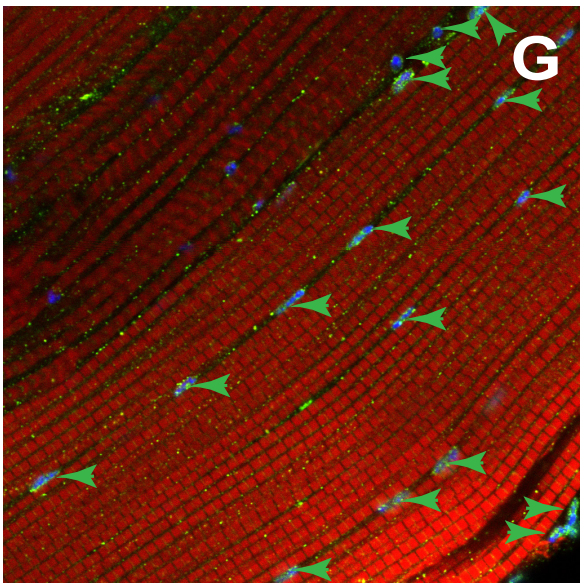
G

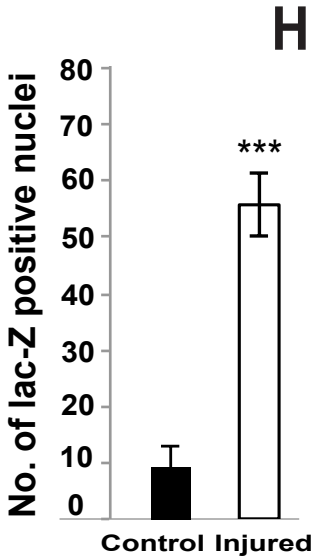
H
No. of lac-Z positive nuclei
80
70
60
50
40
30
20
10
0
***
Control
Injured

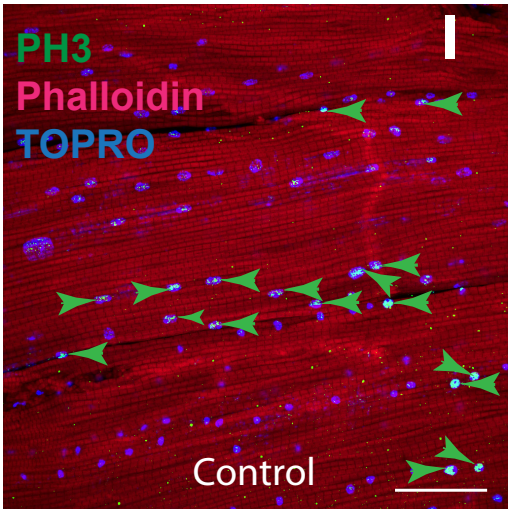
PH3
Phalloidin
TOPRO
I
Control

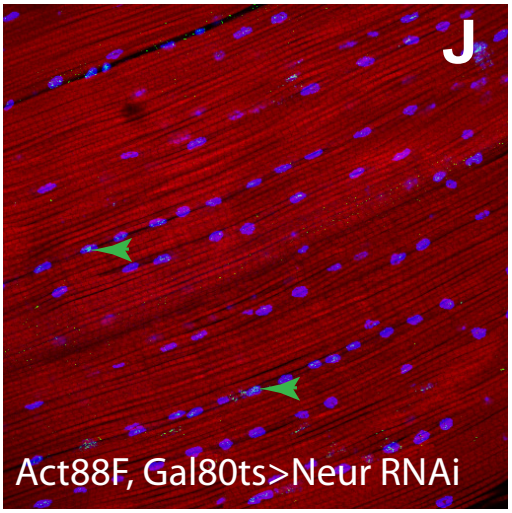
J
Act88F, Gal80ts>Neur RNAi

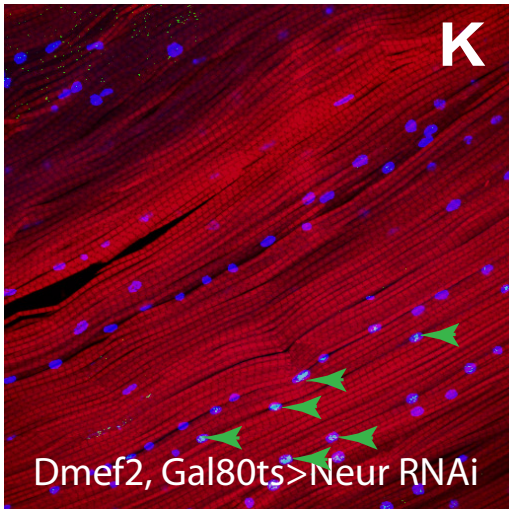
K
Dmef2, Gal80ts>Neur RNAi

Figure 7

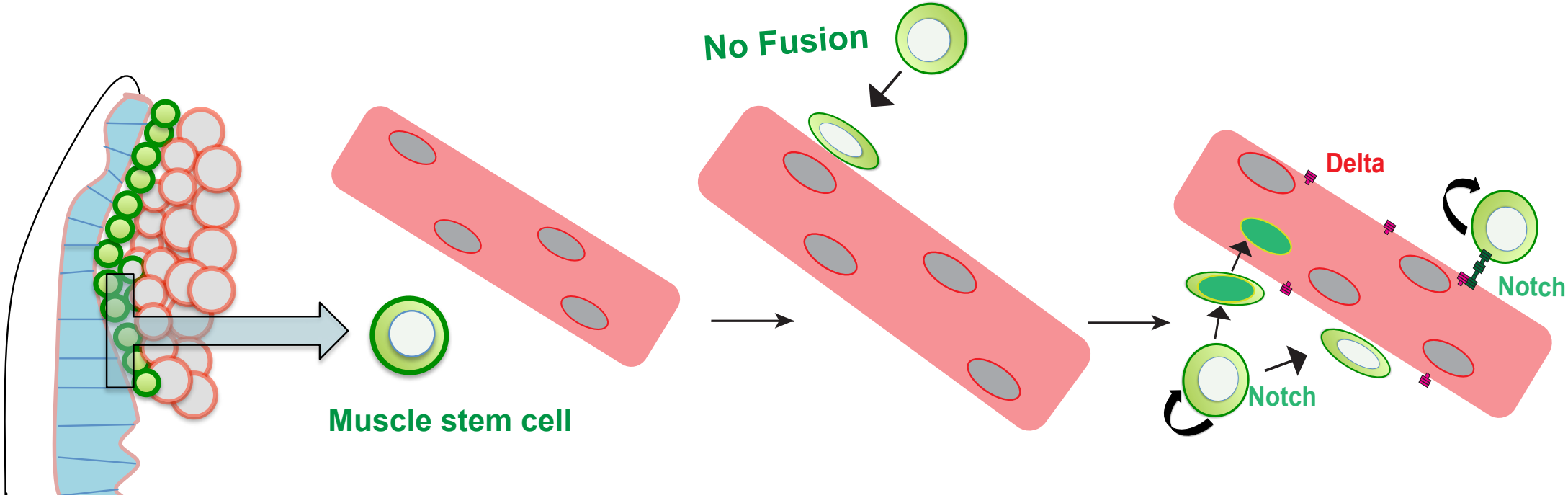

Figure - Unfused cells are devoid of Act88F and Tropomyosin expression

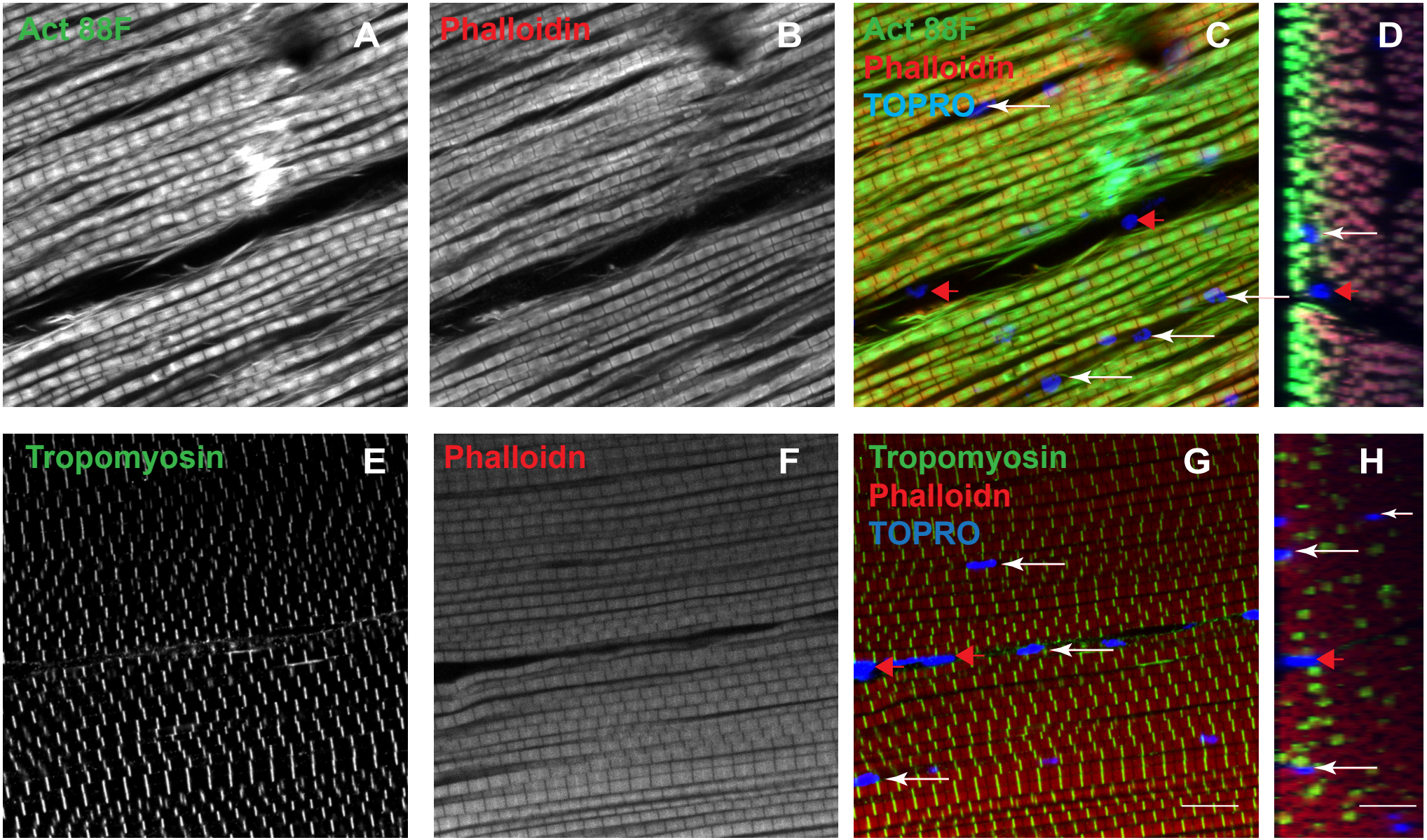

Figure 3 supplement 1

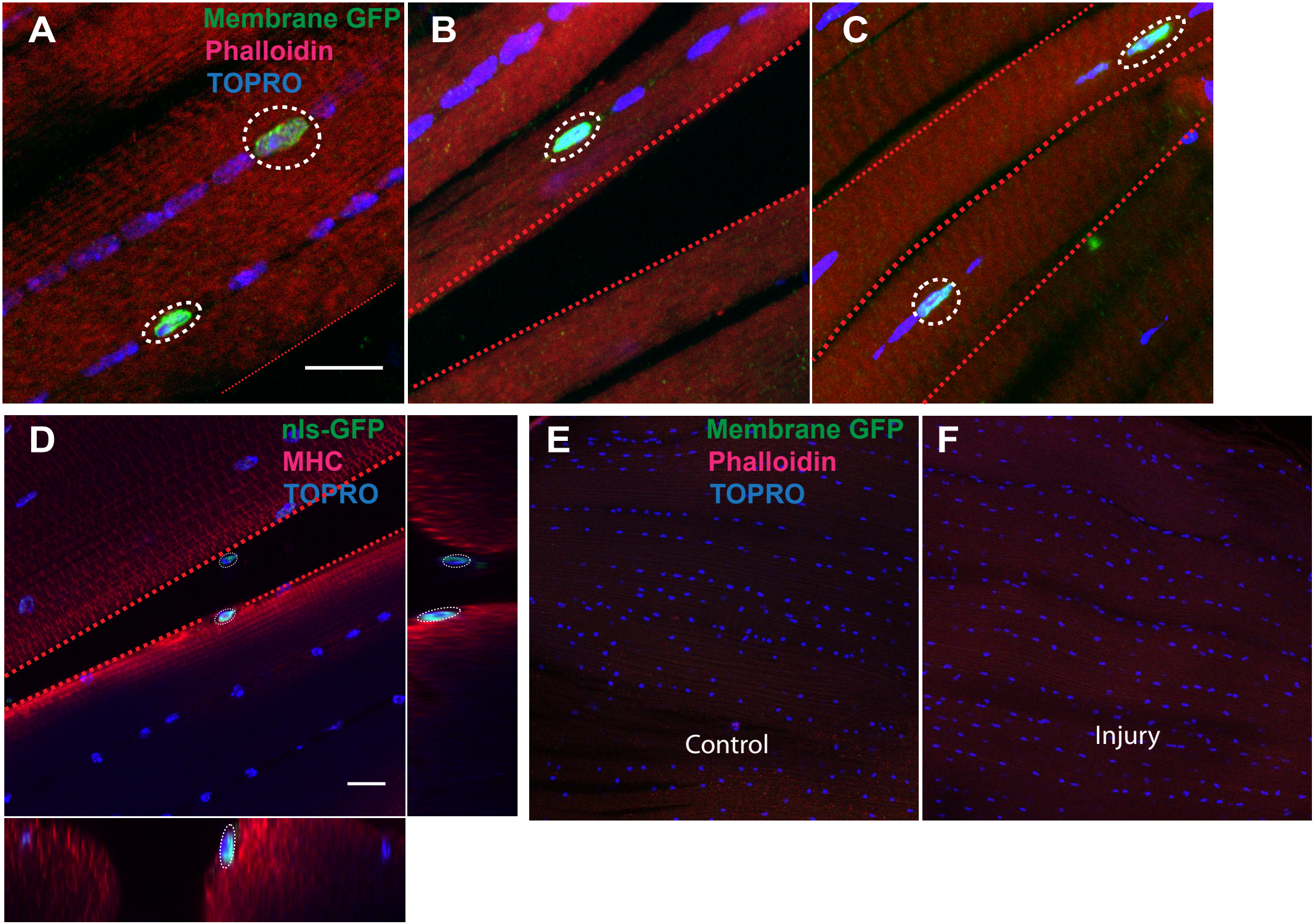

Figure 4 supplement 1

Figure - Recovery of injured muscle after injury

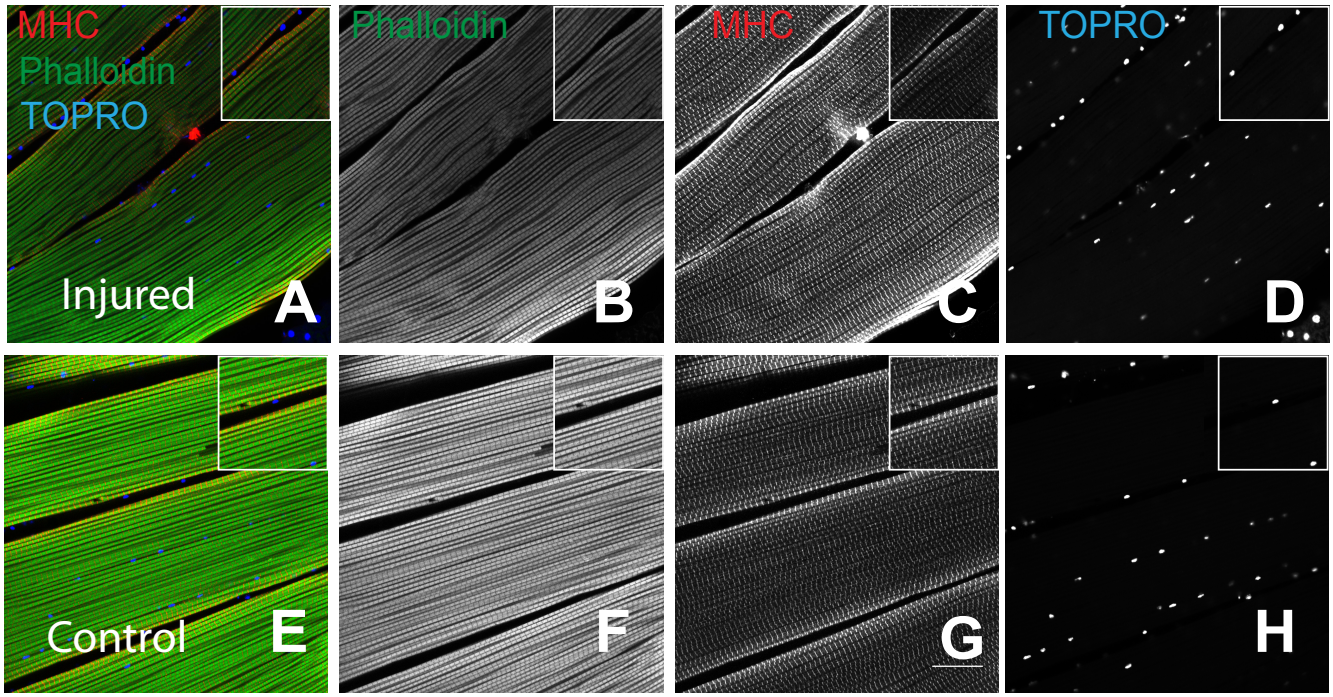

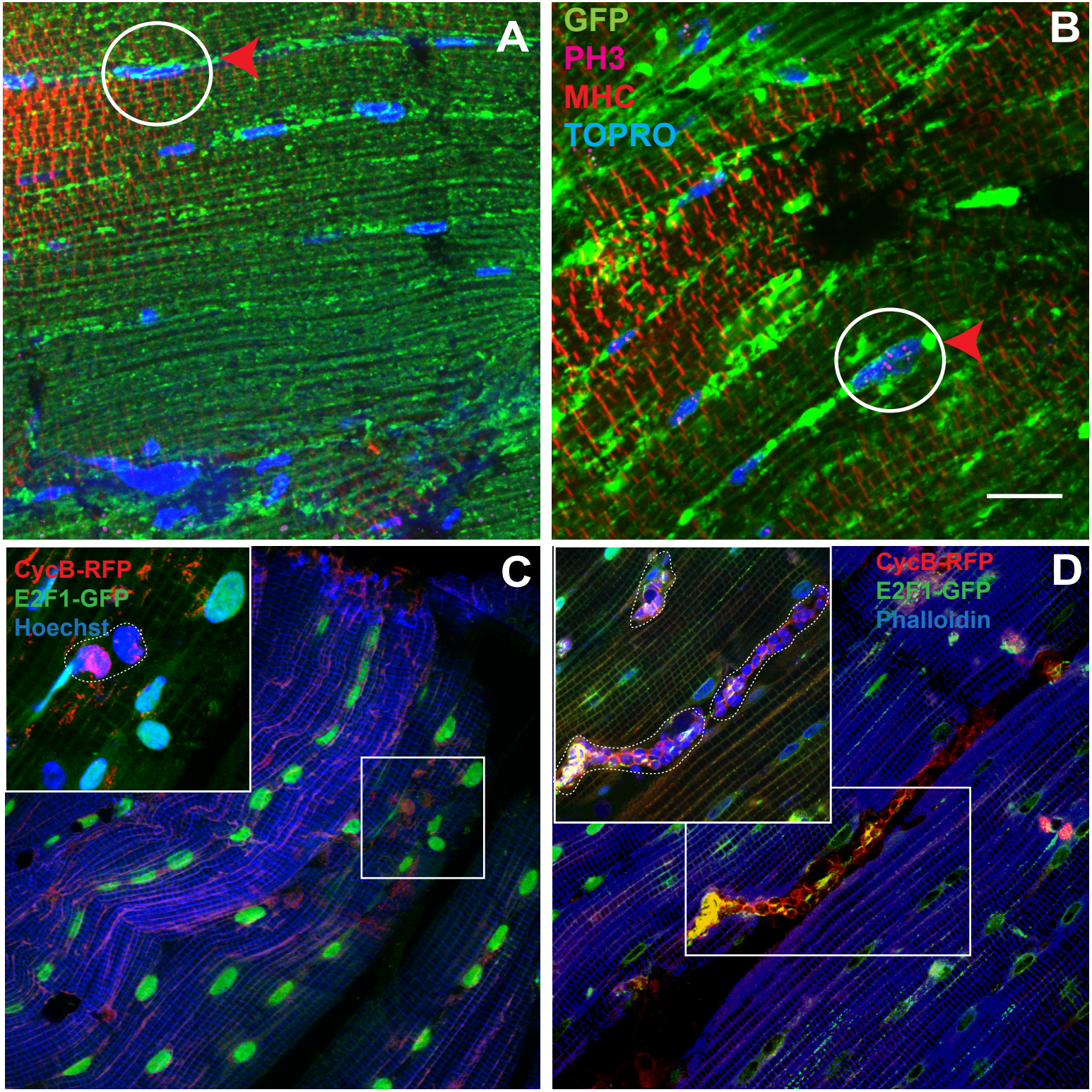

Figure 4 supplement 2

Figure - Notch signaling downregulation using RNAi

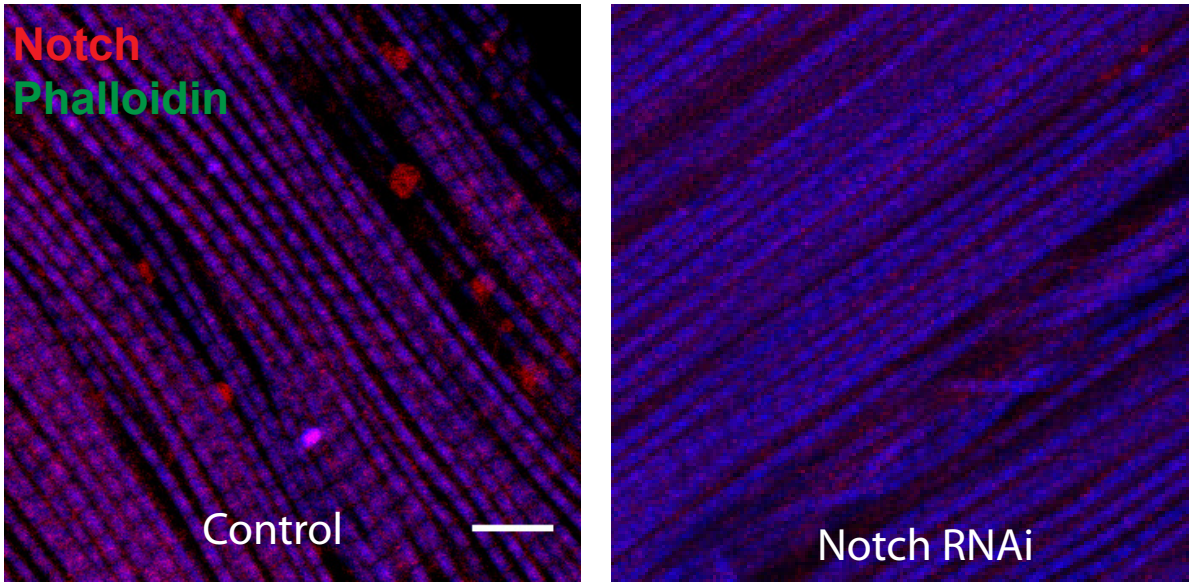
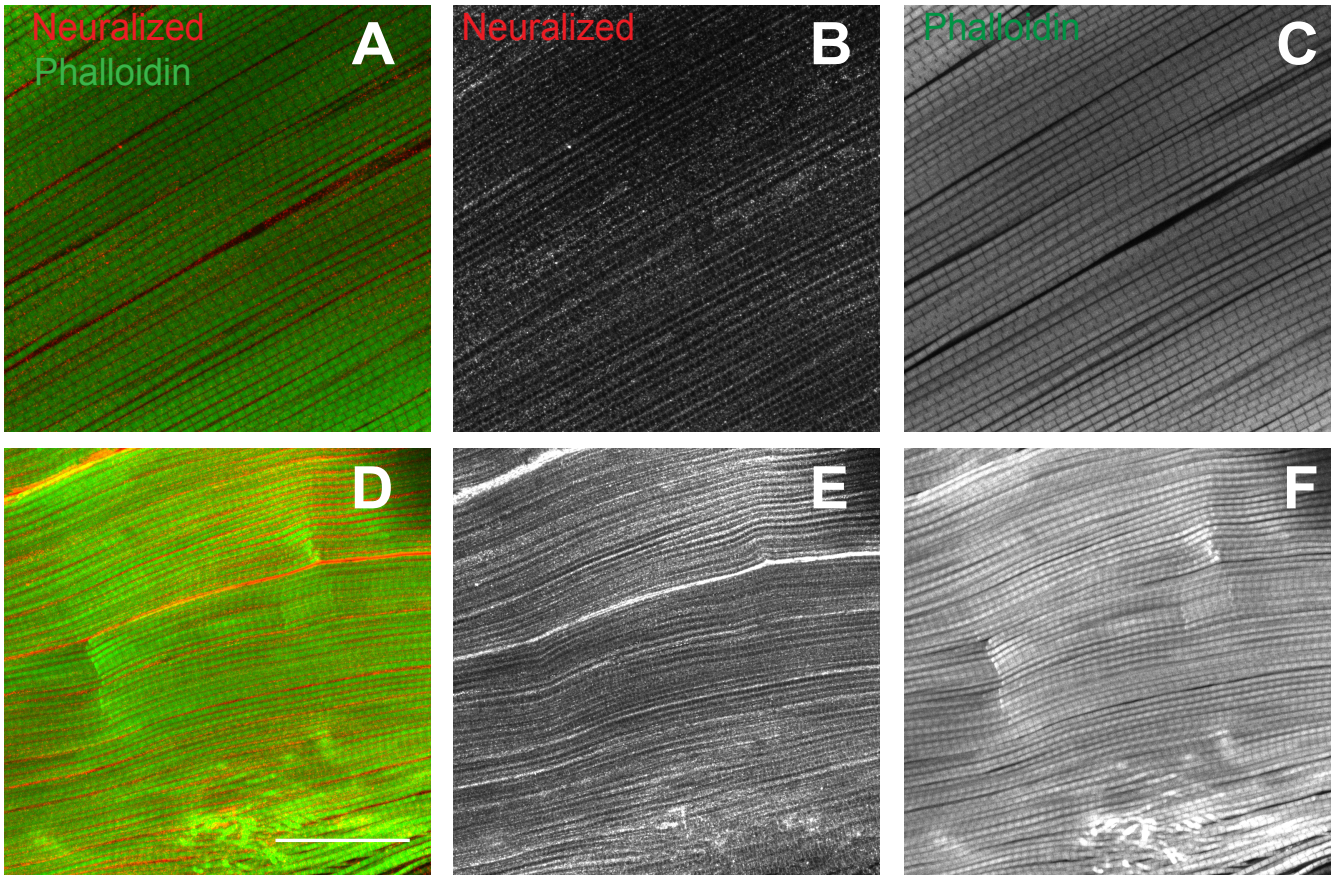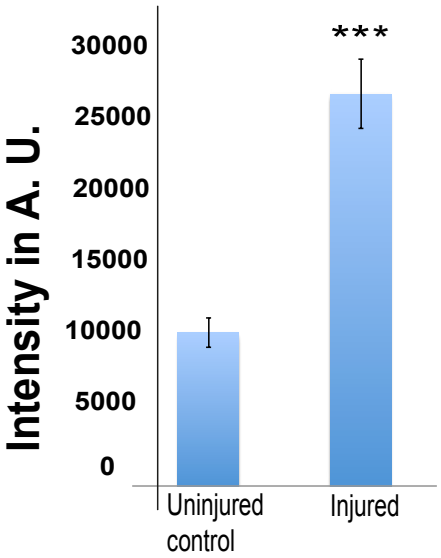
Figure 6 supplement 1